

# A Diagonal Sweeping Domain Decomposition Method with Trace Transfer for the Helmholtz Equation

Wei Leng<sup>a,1</sup>, Lili Ju<sup>b,2,\*</sup>

<sup>a</sup>*Laboratory of Scientific and Engineering Computing, Chinese Academy of Sciences, Beijing 100190, China*

<sup>b</sup>*Department of Mathematics, University of South Carolina, Columbia, SC 29208, USA*

---

## Abstract

In this paper, the diagonal sweeping domain decomposition method (DDM) [26] for solving the high-frequency Helmholtz equation in  $\mathbb{R}^n$  is re-proposed with the trace transfer method [37], where  $n$  is the dimension. The diagonal sweeping DDM [26] uses  $2^n$  sweeps of diagonal directions on the checkerboard domain decomposition based on the source transfer method [7], it is sequential in nature yet suitable for parallel computing, since the number of sequential steps is quite small compared to the number of subdomains. The advantages of changing the basic transfer method from source transfer to trace transfer are as follows: first, no overlapping region is required in the domain decomposition; second, the sweeping algorithm becomes simpler since the transferred traces have only  $n$  cardinal directions, whereas the transferred sources have all  $3^n - 1$  directions. We proved that the exact solution is obtained with the proposed method in the constant medium case, and also in the two-layered medium case provided the source is on the same side with the first swept subdomain. The efficiency of the proposed method is demonstrated using numerical experiments in two and three dimensions, and it is found that numerical differences of the diagonal sweeping DDM with the two transfer methods are very small using second-order finite difference discretization.

**Keywords:** Helmholtz equation, domain decomposition method, diagonal sweeping, perfectly matching layer, trace transfer, parallel computing

---

## 1. Introduction

In this paper, a new domain decomposition method is introduced for the Helmholtz problem in the full space of  $\mathbb{R}^n$  ( $n = 2, 3$ ) with Sommerfeld radiation condition:

$$\Delta u + k^2 u = f, \quad \text{in } \mathbb{R}^n \quad (1)$$

$$r^{\frac{n-1}{2}} \left( \frac{\partial u}{\partial r} - ik u \right) \rightarrow 0, \quad \text{as } r = |\mathbf{x}| \rightarrow \infty, \quad (2)$$

---

\*Corresponding author

Email addresses: [w leng@lsec.cc.ac.cn](mailto:w leng@lsec.cc.ac.cn) (Wei Leng), [ju@math.sc.edu](mailto:ju@math.sc.edu) (Lili Ju)

<sup>1</sup>W. Leng's research is partially supported by Natural Science Foundation of China under grant number 11501553 and the National Center for Mathematics and Interdisciplinary Sciences of Chinese Academy of Sciences.

<sup>2</sup>L. Ju's research is partially supported by US National Science Foundation under grant number DMS-1818438.

where  $k(\mathbf{x})$  is the wave number and defined by  $k(\mathbf{x}) := \omega/c(\mathbf{x})$  with  $\omega$  denoting the angular frequency and  $c(\mathbf{x})$  the wave speed. The Helmholtz equation has varies applications, including acoustics, elasticity, electromagnetics and geophysics. The main computation of these applications involves solving the discrete system of the Helmholtz equation, however, it is hard to find an efficient and robust solver for the Helmholtz equation especially for large wave number, since the discrete system is highly indefinite and the Green's function of the Helmholtz operator is quite oscillatory [16].

Many numerical methods have been developed to solve the discrete system of the Helmholtz equation, including the direct methods [13, 22] with the sparsity of the matrix exploited [36], the multigrid method with the shifted Laplace as the preconditioner [19, 17, 18, 34, 30, 2], the domain decomposition method with different transmission conditions [10, 9, 21, 11, 4, 29, 33], and in this paper we focus on the DDM for the Helmholtz problem.

The sweeping type DDM is first proposed by Engquist and Ying in [14, 15], and then further developed in [31, 35, 37, 7, 20]. The sweeping type DDMs are very effective to solve the Helmholtz problem using two ingredients, the first is employing the PML boundary condition on each subdomain, and the second is the correct transmission conditions between subdomains, which are the main differences between these DDMs. In the sweeping type DDMs, the domain is partitioned into layers in one direction, and the layered subdomain problems are solved one after another in the forward and backward sweeps. The subdomain problem is preferred to be solved with the direct method, which greatly reduces the computation cost in the sweeps, however, the factorization of the direct method for the subdomain problem is computationally expensive in the 3D case.

To overcome the difficulty brought by the one dimensional partition in the sweeping type DDMs, the structured subdomains along all spatial directions (i.e., checkerboard domain decomposition) are then under consideration. One obvious way to build the sweep DDM for the checkerboard partition is to use recursion as in [28, 12], however, the sequential steps in the recursive sweeping is proportional to number of subdomains, thus not practical for real applications.

Inspired by the source trace method [7], the corner directional transfer for the checkerboard domain decomposition is first introduced in the additive overlapping DDM [25]. Following this work, the L-sweeps method [32] are proposed base on the corner directional transfer, sweeps of  $2^n - 1$  directions are performed to construct the total solution, where  $n$  is the dimension, and the sequential steps in the method is reduced to be proportional to the  $n$ -th root of the number of subdomains, thus the method is suitable for parallel computing. The diagonal sweeping DDM with source transfer is then proposed in [26], only diagonal sweep are need in the method instead of all direction sweeps in L-sweeps method, meanwhile the reflections in the medium is handled more properly. In this paper, we re-propose the diagonal sweeping DDM with trace transfer other than source transfer. The overlapping of subdomains is optional for trace transfer method, while it is essential for the source transfer method. Moreover, the DDM with trace transfer is simpler, since the transferred traces are of only cardinal directional, while the transferred sources are of all directional. We proved that the DDM solution is indeed the solution to the problem, in the case of constant medium, and also in the case of two-layered medium if the source position satisfies certain conditions.

The rest of the paper is organized as follows. In Section 2, the trace transfer technique is first reviewed, then the diagonal sweeping DDM with trace transfer in  $\mathbb{R}^2$  is proposed, and we prove that the DDM solutions are exactly the solutions of the PML problems in the constant medium case. Then the proposed method in the two-layered medium case is studied, and the exactness of the DDM solutions is proved under certain conditions on sources in section 3. The extension of

the diagonal sweeping DDM with trace transfer to  $\mathbb{R}^3$  are presented in Section 4. Using extensive numerical experiments in  $\mathbb{R}^2$  and  $\mathbb{R}^3$ , we verify the convergence of the method both in constant and two-layered medium case and demonstrate the efficiency and effectiveness of the method as a preconditioner in Section 5. Finally, some concluding remarks are drawn in Section 6.

## 2. The diagonal sweeping DDM with trace transfer in $\mathbb{R}^2$

In this section, first the Perfect Match Layer (PML) formulation for the Helmholtz equation is recalled and the trace transfer technique is stated, then the diagonal sweeping DDM with trace transfer is proposed in  $\mathbb{R}^2$ , finally the DDM solution is proved to be exact in the constant medium case.

### 2.1. PML and trace transfer

Suppose the source  $f$  is supported in a rectangular box in  $\mathbb{R}^2$  defined as  $B = \{(x_1, x_2)^T : a_j \leq x_j \leq b_j, j = 1, 2\}$ , then the Sommerfeld radiation condition (2) in  $\mathbb{R}^2$  could be replaced by the PML boundary outside the box, and the solution to the Helmholtz equation (1) in  $\mathbb{R}^2$  can still be obtained inside the box. We adopt the uniaxial PML [3, 8, 24, 5, 7], and use the PML medium profile defined as follows. Let  $\{\sigma_j\}_{j=1}^2$  be piecewise smooth functions such that

$$\sigma_j(x) = \begin{cases} \widehat{\sigma}(x_j - b_j), & \text{if } b_j \leq x_j, \\ 0, & \text{if } a_j < x_j < b_j, \\ \widehat{\sigma}(a_j - x_j), & \text{if } x_j \leq a_j, \end{cases} \quad (3)$$

where  $\widehat{\sigma}(t)$  is a smooth medium profile function, then the complex coordinate stretching  $\tilde{\mathbf{x}}(\mathbf{x})$  for  $\mathbf{x} = (x_1, x_2)$  is defined as

$$\tilde{x}_j(x_j) = c_j + \int_{c_j}^{x_j} \alpha_j(t) dt = x_j + \mathbf{i} \int_{c_j}^{x_j} \sigma_j(t) dt, \quad j = 1, 2, \quad (4)$$

where  $c_j = \frac{a_j + b_j}{2}$ , for  $j = 1, 2$ , and  $\alpha_1(x_1) = 1 + \mathbf{i}\sigma_1(x_1)$ ,  $\alpha_2(x_2) = 1 + \mathbf{i}\sigma_2(x_2)$ . The PML equation can be derived from (1) by using the chain rule,

$$J_B^{-1} \nabla \cdot (A_B \nabla \tilde{u}) + k^2 \tilde{u} = f, \quad \text{in } \mathbb{R}^2, \quad (5)$$

where  $\tilde{u}$  is the PML solution and

$$A_B(x) = \text{diag} \left( \frac{\alpha_2(x_2)}{\alpha_1(x_1)}, \frac{\alpha_1(x_1)}{\alpha_2(x_2)} \right), \quad J_B(x) = \alpha_1(x_1)\alpha_2(x_2).$$

It has been prove in [6, 7] that the PML equation (5) is well-posed and the PML solution decays exponentially outside the box, both in the constant medium and also the two-layered medium case.

From now on, the PML problem (5) associated with a rectangular box  $B$  is denoted by  $\mathcal{P}_B$ , and the linear operator associated with  $\mathcal{P}_B$  is denote by  $\mathcal{L}_B := J_B^{-1} \nabla \cdot (A_B \nabla \cdot) + k^2$ . The fundamental solution of  $\mathcal{P}_B$  is denoted as  $G_B(x, y)$ , which satisfies  $\mathcal{L}_B G_B(x, y) = -\delta_y(x)$ . Note that it is proved in [27] that  $G_B(y, x)$  is the fundamental solution to the adjoint PML equation, and it is shown that

$$G_B(y, x) = \frac{J_B(x)}{J_B(y)} G_B(x, y). \quad (6)$$

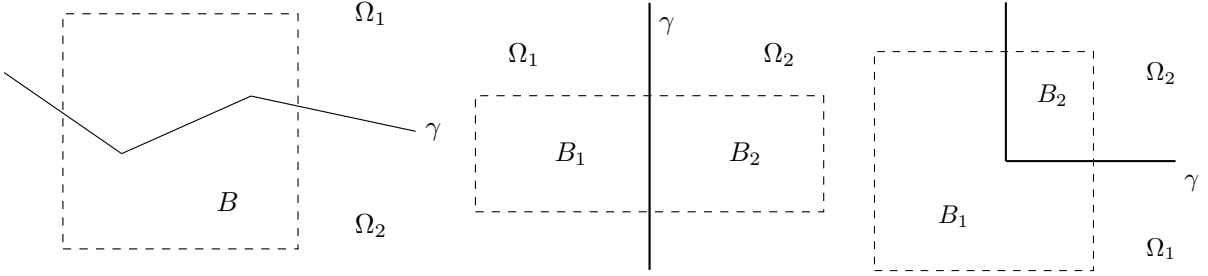


Figure 1: Divide  $\mathbb{R}^2$  and the box  $B$  with  $\gamma$ .

The trace transfer technique used in the polarized trace method is stated as follows. Suppose a piecewise smooth curve  $\gamma$  divides  $\mathbb{R}^2$  into two parts  $\Omega_1$  and  $\Omega_2$ , and also divides the rectangular box  $B$  into two parts, as is shown in Figure 1 (left). Define the discontinuous cutoff function  $\mu_{\Omega'}$  associated with a region  $\Omega'$  as

$$\mu_{\Omega'}(x) = \begin{cases} 1, & \text{if } x \in \Omega' \setminus \partial\Omega', \\ 1/2, & \text{if } x \in \partial\Omega', \\ 0, & \text{if } x \notin \Omega' \cup \partial\Omega', \end{cases}$$

which is the counterpart of the smooth cutoff function in the source transfer technique. Base on the exponential decay of the fundamental solution to the PML problem, we have the following Lemma on trace transfer technique,

**Lemma 2.1.** *Suppose the support of  $f$  is in  $\Omega_1 \cap B$ . Let  $u$  be the solution to the problem  $\mathcal{P}_B$  with the source  $f$  (i.e.,  $\mathcal{L}_B u = f$  in  $\mathbb{R}^2$ ), and let  $u_2$  be the potential using the transferred trace of  $u$  on  $\gamma$ , defined as*

$$u_2 := \int_{\gamma} J_B^{-1} G_B(x, y) (A_B \nabla u(y) \cdot \mathbf{n}) - u(y) \left( A_B \nabla (J_B^{-1} G_B(x, y)) \cdot \mathbf{n} \right) dy, \quad (7)$$

where  $G_B(x, y)$  is the fundamental solution of  $\mathcal{P}_B$  and  $\mathbf{n}$  is the normal of  $\gamma$  pointing to  $\Omega_2$ . Then we have that

$$u \mu_{\Omega_1} + u_2 \mu_{\Omega_2} = u, \quad \text{in } \mathbb{R}^n, \quad (8)$$

where  $n = 2, 3$ . Moreover,  $u_2 = 0$  in  $\Omega_1 \setminus \gamma$ .

**Remark 1.** *The following convention is used for the potential integral (7) throughout this paper: the function  $u$  and its derivative in the integrand on  $\gamma$  is defined as their limits from the positive  $n$  side, and the value of the integral on  $\gamma$  is also defined as its limits from the positive  $n$  side.*

Similar to the diagonal source transfer method, the Lemma 2.1 is applied in DDM for horizontal or vertical interfaces and quadrant region interfaces, as is shown in Figure 1 (middle and right). The Lemma 2.1 of trace transfer implies a procedure of two subdomains solving, suppose we only know the solution in  $\Omega_1$ , and smoothly extend it to  $\Omega_2$ , then the solution in  $\Omega_2$  could be obtained using potential (7), together they form the total solution with (8). Building a domain decomposition method further requires to change the global problem solving in the procedures to subdomain problems solving, that is, substitute the fundamental solution  $G_B(x, y)$  of global domain in (7) to

the ones of subdomains. Assume that  $\Omega_2 \cap B$  is also a rectangular, which is denoted by  $B_2$ , then the subdomain PML problem for  $B_2$  could be built, however, the wave number of the subdomain problem, which is denoted by  $k_2$ , could be different from  $k$ . We have the following lemma,

**Lemma 2.2.** *Suppose  $f$  and  $u$  satisfies the conditions in Lemma 2.1. Assume that the wave number  $k_2$  satisfies the following two conditions: (i)  $k_2 = k$  in  $\Omega_2$ , (ii)  $k_2$  is either constant, or two layered in horizontal or vertical direction. Let  $\tilde{u}_2$  be the potential associated with the subdomain PML problem of  $B_2$  with wave number  $k_2$ , defined as*

$$\tilde{u}_2 := \int_{\gamma} J_{B_2}^{-1} G_{B_2}(x, y) (A_{B_2} \nabla u(y) \cdot \mathbf{n}) - u(y) (A_{B_2} \nabla (J_{B_2}^{-1} G_{B_2}(x, y)) \cdot \mathbf{n}) dy, \quad (9)$$

then  $\tilde{u}_2 = u_2$  in  $\mathbb{R}^2$ .

*Proof.* By the definition of uPML, it is clear that  $J_{B_2} = J_B$  and  $A_{B_2} = A_B$  on  $\gamma$ , and also  $G_{B_2}(x, y) = G_B(x, y)$  for  $x \in \Omega_2$ ,  $y \in \gamma$ , thus  $\tilde{u}_2 = u_2$  in  $\Omega_2$ . Since  $u_2 = 0$  in  $\Omega_1$ , we will show that  $\tilde{u}_2 = 0$  in  $\Omega_1$  using the source transfer argument as follows.

We define  $\Omega_2^\varepsilon := \{x | \rho(x, \Omega_2) \leq \varepsilon\}$ , which is an extended region of  $\Omega_2$  by a distance of  $\varepsilon$ , and let  $\Omega^\varepsilon = \Omega_2^\varepsilon \setminus \Omega_2$ . A smooth function  $\beta^\varepsilon$  exists such that  $\beta^\varepsilon = 1$  in  $\Omega_1 \setminus \Omega^\varepsilon$ , and  $\beta^\varepsilon = 0$  in  $\Omega_2$ . Denote  $u^\varepsilon$  as the solution to problem  $\mathcal{P}_B$  with the source  $f \cdot \chi_{\Omega_1 \setminus \Omega^\varepsilon}$ , and  $v^\varepsilon$  as the solution to the following problem,

$$\mathcal{L}_B v^\varepsilon = -\mathcal{L}_B(u^\varepsilon \beta^\varepsilon) \chi_{\Omega^\varepsilon}, \quad \text{in } \mathbb{R}^2, \quad (10)$$

then clearly

$$\mathcal{L}_B v^\varepsilon = f - \mathcal{L}_B(u^\varepsilon \beta^\varepsilon), \quad \text{in } \mathbb{R}^2,$$

which imples

$$v^\varepsilon = u^\varepsilon(1 - \beta^\varepsilon), \quad \text{in } \mathbb{R}^2. \quad (11)$$

Let the extended rectangular of  $B_2$  be defined as  $B_2^\varepsilon = \Omega_2^\varepsilon \cap B$ , then by (10) and (11), it is shown that  $v^\varepsilon$  is also the solution to the following subdomain problem associated with  $B_2^\varepsilon$ ,

$$\mathcal{L}_{B_2^\varepsilon} v^\varepsilon = -\mathcal{L}_B(u^\varepsilon \beta^\varepsilon) \chi_{\Omega^\varepsilon}, \quad \text{in } \mathbb{R}^2. \quad (12)$$

Using Lemma 2.1 on the problem (12), we have that for  $x \in \Omega_1$ ,

$$\int_{\gamma} J_{B_2^\varepsilon}^{-1} G_{B_2^\varepsilon}(x, y) (A_{B_2^\varepsilon} \nabla u^\varepsilon(y) \cdot \mathbf{n}) - u^\varepsilon(y) (A_{B_2^\varepsilon} \nabla (J_{B_2^\varepsilon}^{-1} G_{B_2^\varepsilon}(x, y)) \cdot \mathbf{n}) dy = 0, \quad (13)$$

where we have used the fact that  $u^\varepsilon = v^\varepsilon$  on  $\gamma$ . Clearly,  $J_{B_2^\varepsilon} = J_{B_2}$ ,  $A_{B_2^\varepsilon} = A_{B_2}$  on  $\gamma$ . By the well-posedness of the PML problem, we know that  $\lim_{\varepsilon \rightarrow 0} u^\varepsilon(y) = u(y)$ , and  $\lim_{\varepsilon \rightarrow 0} \nabla u^\varepsilon = \nabla u$  on  $\gamma$ . Moreover, by the properties of the fundamental solution with the wave number  $k_2$ , for  $x \in \Omega_1$  and  $y \in \gamma$ , we have that  $\lim_{\varepsilon \rightarrow 0} G_{B_2^\varepsilon}(x, y) = G_{B_2}(x, y)$ , and  $\lim_{\varepsilon \rightarrow 0} \nabla (J_{B_2^\varepsilon}^{-1} G_{B_2^\varepsilon}(x, y)) = \nabla (J_{B_2}^{-1} G_{B_2}(x, y))$ . Therefore we have that for  $x \in \Omega_1$ ,

$$\int_{\gamma} J_{B_2}^{-1} G_{B_2}(x, y) (A_{B_2} \nabla u(y) \cdot \mathbf{n}) - u(y) (A_{B_2} \nabla (J_{B_2}^{-1} G_{B_2}(x, y)) \cdot \mathbf{n}) dy = 0, \quad (14)$$

that is,  $\tilde{u}_2 = 0$  in  $\Omega_1$ . This completes the proof.  $\square$

We use the following domain decomposition of the rectangular domain  $\Omega = (-l_1, l_1) \times (-l_2, l_2)$  in  $\mathbb{R}^2$ . Denote  $\Delta\xi = 2l_1/N_1$ ,  $\xi_i = -l_1 + (i-1)\Delta\xi$  for  $i = 1, 2, \dots, N_1 + 1$ , and  $\Delta\eta = 2l_2/N_2$ ,  $\eta_j = -l_2 + (j-1)\Delta\eta$  for  $j = 1, 2, \dots, N_2 + 1$ , then the  $N_1 \times N_2$  nonoverlapping rectangular subdomains are

$$\Omega_{i,j} := [\xi_i, \xi_{i+1}] \times [\eta_j, \eta_{j+1}], \quad i = 1, 2, \dots, N_1, j = 1, 2, \dots, N_2.$$

We define  $\Omega_{i0, i1; j0, j1}$ ,  $1 \leq i0 \leq i1 \leq N_1 + 1$ ,  $1 \leq j0 \leq j1 \leq N_2 + 1$ , as the union of the subdomains as follows:

$$\Omega_{i0, i1; j0, j1} := \bigcup_{\substack{i0 \leq i \leq i1 \\ j0 \leq j \leq j1}} \Omega_{i,j}.$$

The decomposition of the source  $f$  is defined as

$$f_{i,j} = f \cdot \chi_{\Omega_{i,j}}, \quad i = 1, 2, \dots, N_1, j = 1, 2, \dots, N_2.$$

The PML problem  $\mathcal{P}_{\Omega_{i,j}}$  for the subdomain  $\Omega_{i,j}$  uses a wavenumber denoted as  $k_{i,j}$ , which is defined as the extension of the subdomain interior wavenumber, namely,

$$k_{i,j}(x) = k(x'^+), \quad (15)$$

where  $x' = \arg \min_{y \in \Omega_{i,j}} \rho(x, y)$  and  $x'^+$  stands for the limit from outside of the subdomain. With this definition, the subdomain lying in the interior of one medium will have a constant wave number. We note that in the special case that the layered medium interface coincides with the interface of two subdomains, both the subdomains will have the wave number of the layered medium.

## 2.2. Diagonal sweeping for the constant problem

The following notations are introduced. Define the one-dimensional cutoff functions as,

$$\mu_{\square; i}^{(1)}(x_1) = \begin{cases} H(\xi_i - x_1), & \square = -1, \\ H(x_1 - \xi_{i+1}), & \square = 1, \end{cases} \quad \mu_{\Delta; j}^{(2)}(x_2) = \begin{cases} H(\eta_j - x_2), & \Delta = -1, \\ H(x_2 - \eta_{j+1}), & \Delta = 1, \end{cases}$$

for  $i = 1, \dots, N_1$ ,  $j = 1, \dots, N_2$ , and the two-dimensional cutoff functions as

$$\mu_{i,j}(x_1, x_2) = \mu_{-1; i}^{(1)}(x_1) \mu_{+1; i}^{(1)}(x_1) \mu_{-1; j}^{(2)}(x_2) \mu_{+1; j}^{(2)}(x_2).$$

These cutoff functions are the discontinuous counterpart of the smooth cutoff functions in the diagonal sweeping DDM with source transfer. Denote by  $G_{i,j}(x, y)$  the fundamental solution to the problem  $\mathcal{P}_{\Omega_{i,j}}$ , and define the four boundaries of  $\Omega_{i,j}$  as

$$\gamma_{\square, \Delta; i, j} = \begin{cases} \{(x_1, x_2) | x_1 = \xi_i\}, & \text{if } (\square, \Delta) = (-1, 0) \text{ and } i > 1 \\ \{(x_1, x_2) | x_1 = \xi_{i+1}\}, & \text{if } (\square, \Delta) = (+1, 0) \text{ and } i < N_1 \\ \{(x_1, x_2) | x_2 = \eta_j\}, & \text{if } (\square, \Delta) = (0, -1) \text{ and } j > 1 \\ \{(x_1, x_2) | x_2 = \eta_{j+1}\}, & \text{if } (\square, \Delta) = (0, +1) \text{ and } j < N_2 \\ \emptyset, & \text{otherwise,} \end{cases}$$

where  $(\square, \Delta) = (\pm 1, 0), (0, \pm 1)$ , and the normal direction associated with them are defined as  $\mathbf{n}_{\square, \Delta} = -(\square, \Delta)$ . Using the above cutoff functions and fundamental solutions, we are able to define the potential operators as follows:

$$\Phi_{\square, \Delta; i, j}((v, w)^T) := \int_{\gamma_{\square, \Delta; i, j}} J_{i, j}^{-1} G_{i, j}(x, y) w(y) \quad (16)$$

$$- v(y) \left( A_{i, j} \nabla_y (J_{i, j}^{-1} G_{i, j}(x, y)) \cdot \mathbf{n}_{\square, \Delta} \right) dy \quad (17)$$

and

$$\Psi_{\square, \Delta; i, j}(v) = \Phi_{\square, \Delta; i, j}((v, A_{i, j} \nabla v \cdot \mathbf{n}_{\square, \Delta})^T) \quad (18)$$

where  $(\square, \Delta) = (\pm 1, 0), (0, \pm 1)$ .

Four diagonal sweeping directions are used in the 2D diagonal sweeping method, which are  $(\square, \Delta)$ ,  $\square, \Delta = \pm 1$ , and the sweeping order is the same with [26], that is,

$$(+1, +1), \quad (-1, +1), \quad (+1, -1), \quad (-1, -1). \quad (19)$$

Defining that two vectors  $\mathbf{d}_1$  and  $\mathbf{d}_2$  in  $\mathbb{R}^2$  are in the similar direction if  $\mathbf{d}_1 \cdot \mathbf{d}_2 > 0$ , the following rules on the transferred sources in sweeps in  $\mathbb{R}^2$  are introduced, which is also the same with [26].

**Rule 2.3.** (Similar directions in  $\mathbb{R}^2$ ) *A transferred trace which is not in the similar direction of one sweep in  $\mathbb{R}^2$ , should not be used in that sweep.*

**Rule 2.4.** (Opposite directions in  $\mathbb{R}^2$ ) *The transferred trace generated in one sweep in  $\mathbb{R}^2$  should not be used in a later sweep if these two sweeps have opposite directions.*

The diagonal sweeping DDM with trace transfer in  $\mathbb{R}^2$  is stated as follows.

**Algorithm 2.1** (Diagonal sweeping DDM with trace transfer in  $\mathbb{R}^2$ ).

- 1: Set the sweep order as  $(+1, +1), (-1, +1), (+1, -1), (-1, -1)$
- 2: Set the local trace of each subdomain for each sweep as  $\mathbf{g}_{\square, \Delta; i, j}^l = 0$ ,  $l = 1, 2, 3, 4$
- 3: **for** sweep  $l = 1, \dots, 4$  **do**
- 4:   **for** step  $s = 1, \dots, N_1 + N_2 - 1$  **do**
- 5:     **for** subdomain  $\Omega_{i, j}$  in the step  $s$  of the sweep  $l$  **do**
- 6:       If  $f_{i, j} \neq 0$ , then solve the local solution  $\mathcal{L}_{i, j}(u_{i, j}^l) = f_{i, j}$ ,  
or else set  $u_{i, j}^l = 0$  without solving
- 7:       Set  $f_{i, j} = 0$
- 8:       Add potentials to the local solution

$$u_{i, j}^l += \sum_{(\square, \Delta) = (\pm 1, 0), (0, \pm 1)} \Phi_{\square, \Delta; i, j}(\mathbf{g}_{\square, \Delta; i, j}^l) \quad (20)$$

- 9:       **for** each direction  $(\square, \Delta) = (\pm 1, 0), (0, \pm 1)$  **do**
- 10:         Compute new transferred trace  $\left( u_{i, j}^l, A_{i, j} \nabla u_{i, j}^l \cdot \mathbf{n}_{\square, \Delta} \right)^T \Big|_{\gamma_{\square, \Delta; i, j}}$
- 11:         Find the smallest sweep number  $l' \geq l$ , such that the transferred trace could be used in sweep  $l'$ , according to Rule 2.3 and 2.4

12: *Add the transferred trace to the  $l'$ -th local trace of the corresponding neighbor subdomain*

$$\mathbf{g}_{-\square, -\Delta; i+\square, j+\Delta}^{l'} += \left( u_{i,j}^l, A_{i,j} \nabla u_{i,j}^l \cdot \mathbf{n}_{\square, \Delta} \right)^T \Big|_{\gamma_{\square, \Delta; i,j}}$$

13: *end for*

14: *end for*

15: *end for*

16: *end for*

17: *Summarize the DDM solution as*

$$u_{DDM} = \sum_{l=1, \dots, 4} \sum_{\substack{i=1, \dots, N_1 \\ j=1, \dots, N_2}} u_{i,j}^l \mu_{i,j}$$

We note that the subdomain problem (20) is solved with several potentials, however, in the numerical discretization, these potentials are not computed individually and sum together, instead, the line integrals of the potentials are discretized as sources as in the polarized trace method [37], then the sources are sum as one RHS and solved, therefore the subdomain problem (20) is solved only once in one step.

### 2.3. Verification of the DDM solution

In this subsection, we will verify that the DDM solution in Algorithm 2.1 is exactly the solution to the problem  $\mathcal{P}_\Omega$  with source  $f$ . We start by assuming that the source lies in only one subdomain, i.e.,  $\text{supp}(f) \subset \Omega_{i_0, j_0}$ , and verify the DDM solution in such a case. The subdomain solution construction in the first sweep is considered first, focusing on the application of the cardinal directional and corner directional trace transfer, then the subdomain solution construction in all sweeps is considered, focusing on the movement of the transferred traces in sweeps.

The following notations are introduced for convenience. For the source  $f$  lying in  $\Omega_{i_0, j_0}$ , we can define the regional solution  $u_{i_1, i_2; j_1, j_2}$  as the solution to the problem  $\mathcal{P}_{\Omega_{i_1, i_2; j_1, j_2}}$  with the source  $f$ , where  $i_1 \leq i_0 \leq i_2$  and  $j_1 \leq j_0 \leq j_2$ , obviously,  $u_{i_1, i_2; j_1, j_2} = u$  in  $\Omega_{i_1, i_2; j_1, j_2}$ , where  $u$  is the solution to problem  $\mathcal{P}_\Omega$ .

The cardinal directional and corner directional trace transfers in the subdomain solution construction of the **first sweep** is considered. The nonzero subdomain solve starts at step  $i_0 + j_0 - 1$ , the subdomain problem  $\mathcal{P}_{\Omega_{i_0, j_0}}$  is solved with the source  $f$ , and in the following steps, the subdomain problem  $\mathcal{P}_{\Omega_{i,j}}$ ,  $i \geq i_0$ ,  $j \geq j_0$ , is solved at step  $i + j - 1$ .

For those subdomains to the right of  $\Omega_{i_0, j_0}$ , i.e.,  $\Omega_{i, j_0}$ ,  $i = i_0 + 1, \dots, N_1$ , the subdomain solutions  $u_{i, j_0}^1$  are obtained one per step from left to right. By applying the horizontal trace transfer repeatedly on the region  $\Omega_{i_0, i; j_0, j_0}$ ,  $i = i_0 + 1, \dots, N_1$ , one can show that for  $i' > i_0$ ,

$$\sum_{i=i_0, \dots, i'} u_{i, j_0}^1 \mu_{i, j_0} = u_{i_0, i'; j_0, j_0}, \quad \text{in } \Omega_{i_0, i'; j_0, j_0}. \quad (21)$$

Similarly, for the subdomains on the top of  $\Omega_{i_0, j_0}$ , we have that for  $j' > j_0$ ,

$$\sum_{j=j_0, \dots, j'} u_{i_0, j}^1 \mu_{i_0, j} = u_{i_0, i_0; j_0, j'}, \quad \text{in } \Omega_{i_0, i_0; j_0, j'}. \quad (22)$$

The following lemma holds for the solutions of the subdomains in the upper right direction of the subdomain  $\Omega_{i_0, j_0}$ ,

**Lemma 2.5.** *For the constant medium problem, suppose the source satisfies  $\text{supp}(f) \subset \Omega_{i_0, j_0}$ , then for any  $i' > i_0$  and  $j' > j_0$ , we have*

$$\sum_{\substack{i=i_0, \dots, i' \\ j=j_0, \dots, j'}} u_{i,j}^1 \mu_{i,j} = u_{i_0, i'; j_0, j'} \quad \text{in } \Omega_{i_0, i'; j_0, j'}. \quad (23)$$

*Proof.* First we consider the subdomain  $\Omega_{i_0+1, j_0+1}$ , of which the local problem is solved at step  $i_0 + j_0 + 1$  in the first sweep, as is shown in Figure 2. The local problems of its lower left neighbor subdomain  $\Omega_{i_0, j_0}$  is solved two steps before, as is shown in Figure 3 (a). The local problems of its lower neighbor subdomain  $\Omega_{i_0+1, j_0}$ , and its left neighbor subdomain  $\Omega_{i_0, j_0+1}$ , are solved one step before, as are shown in Figure 3 (b) and (d), respectively. Consequently, for the region  $\Omega_{i_0, i_0+1; j_0, j_0+1}$  with  $2 \times 2$  subdomains, three subdomain problems have been solved and the solutions within have been constructed, while one subdomain problem in the corner direction is left to be solved. For convenience, in this proof we let  $\mu_{\rightarrow} = \mu_{+1; i_0}^{(1)}$ ,  $\mu_{\uparrow} = \mu_{+1; j_0}^{(2)}$ ,  $\mu_{\leftarrow} = \mu_{-1; i_0+1}^{(1)}$ ,  $\mu_{\downarrow} = \mu_{-1; j_0+1}^{(2)}$ ,  $\widehat{\Omega} = \Omega_{i_0, i_0+1; j_0, j_0+1}$ ,  $\widehat{u} = u_{i_0, i_0+1; j_0, j_0+1}$ , and omit the superscripts of the subdomain solutions which indicate the first sweep, i.e.,  $u_{i,j} = u_{i,j}^1$ .

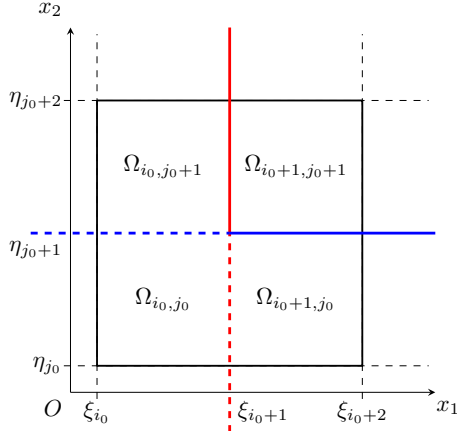


Figure 2: The corner direction trace transfer for solving subdomain problem of  $\Omega_{i_0+1, j_0+1}$ . The red line (solid and dotted) denotes  $\gamma_{-1, 0; i_0+1, j_0+1}$ , the blue line (solid and dotted) denotes  $\gamma_{0, -1; i_0+1, j_0+1}$ , and the solid line (blue and red) denotes  $\gamma_{\rightarrow}$ .

By applying the horizontal direction trace transfer on  $\Omega_{i_0, i_0+1; j_0, j_0}$ , we know that

$$u_{i_0, j_0} \mu_{\rightarrow} + u_{i_0+1, j_0} \mu_{\leftarrow} = \widehat{u}, \quad \text{in } (-\infty, +\infty) \times (-\infty, \eta_{j_0+1}) \quad (24)$$

as is shown in Figure 3 (c). Similarly, we have

$$u_{i_0, j_0} \mu_{\uparrow} + u_{i_0, j_0+1} \mu_{\downarrow} = \widehat{u}, \quad \text{in } (-\infty, \xi_{i_0+1}) \times (-\infty, +\infty) \quad (25)$$

as is shown in Figure 3 (e).

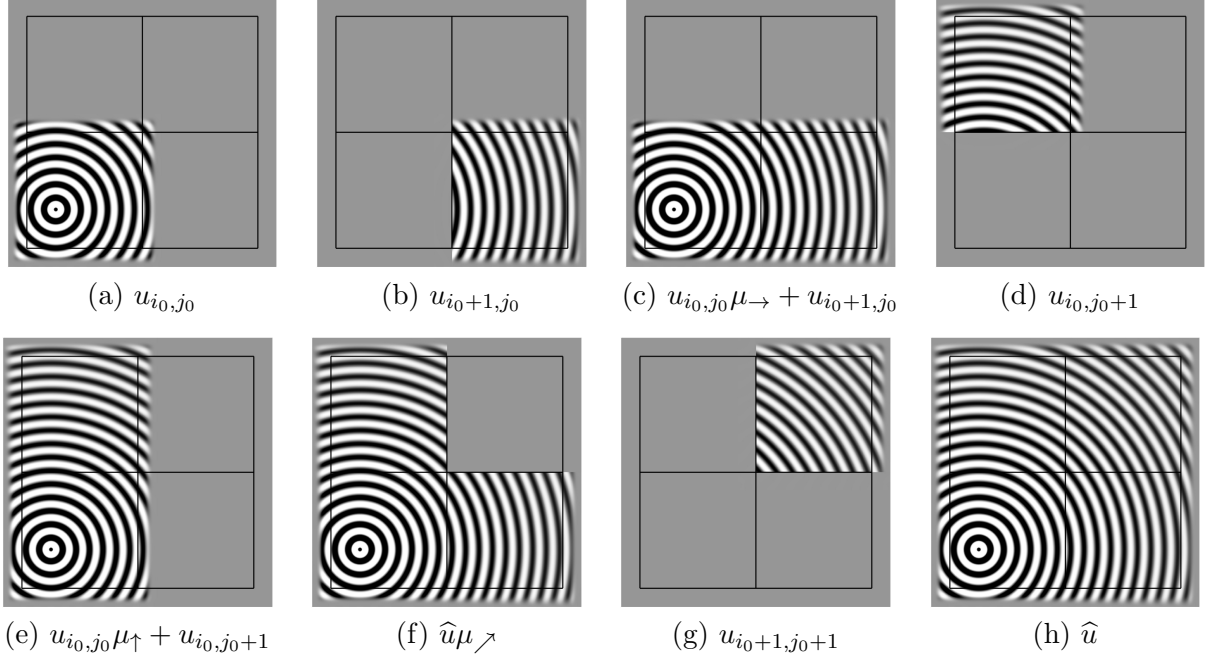


Figure 3: Illustration of the process of source transfer in the upper-right corner direction.

The subdomain problem of  $\Omega_{i_0+1,j_0+1}$  is solved with the upward transferred trace from subdomain  $\Omega_{i_0+1,j_0}$ , and the rightward transferred trace from subdomain  $\Omega_{i_0,j_0+1}$ , by (24), (25) and the fact that  $u_{i_0+1,j_0} = 0$  on  $(-\infty, \xi_{i_0+1}) \times \{\eta_{j_0+1}\}$ , and  $u_{i_0,j_0+1} = 0$  on  $\{\xi_{i_0+1}\} \times (-\infty, \eta_{j_0+1})$ , we show that

$$\begin{aligned} u_{i_0+1,j_0+1} &= \Psi_{0,-1;i_0+1,j_0+1}(u_{i_0+1,j_0}) + \Psi_{-1,0;i_0+1,j_0+1}(u_{i_0,j_0+1}) \\ &= \int_{\gamma_{\nearrow}} J_{i_0+1,j_0+1}^{-1} G_{i_0+1,j_0+1}(x, y) \left( A_{i_0+1,j_0+1} \nabla \hat{u} \cdot \mathbf{n}_{\nearrow} \right) \\ &\quad - \hat{u} \left( A_{i_0+1,j_0+1} \nabla_y (J_{i_0+1,j_0+1}^{-1} G_{i_0+1,j_0+1}(x, y)) \cdot \mathbf{n}_{\nearrow} \right) dy, \end{aligned}$$

where  $\gamma_{\nearrow} = \{(x_1, x_2) | x_1 = \xi_2, x_2 \geq \eta_2 \text{ or } x_1 \geq \xi_2, x_2 = \eta_2\}$ , and  $\mathbf{n}_{\nearrow}$  is the normal of  $\gamma_{\nearrow}$  pointing to  $\Omega_{i_0+1,j_0+1}$ , as shown in Figure 2.

By applying the corner direction trace transfer on  $\widehat{\Omega}$ , we know that

$$\hat{u} \mu_{\nearrow} + u_{i_0+1,j_0+1} \mu_{\leftarrow} - \mu_{\downarrow} = \hat{u}, \quad (26)$$

where  $\mu_{\nearrow} = 1 - (1 - \mu_{\rightarrow})(1 - \mu_{\uparrow})$ , as is shown in Figure 3 (f)-(h). This implies that,

$$u_{i_0,j_0} \mu_{\rightarrow} \mu_{\uparrow} + u_{i_0+1,j_0} \mu_{\uparrow} \mu_{\leftarrow} + u_{i_0,j_0+1} \mu_{\rightarrow} \mu_{\downarrow} + u_{i_0+1,j_0+1} \mu_{\leftarrow} \mu_{\downarrow} = \hat{u},$$

thus we known that (23) holds for the case  $i' = i_0 + 1$  and  $j' = j_0 + 1$ . Note that the upward and rightward transferred traces are then generated from the subdomain  $\Omega_{i_0+1,j_0+1}$ , while both the leftward and downward transferred traces are zero.

Next we prove (23) by induction. We will prove that for any  $s > 0$ , (23) holds for  $i'$  and  $j'$  that  $i' + j' \leq i_0 + j_0 + s$ ,  $i' \geq i_0$ ,  $j' \geq j_0$ . The case that  $s = 1, 2$  has been proved, now

assume (23) holds for  $s \leq t$ , we will prove it also holds for  $s = t + 1$ . For subdomain  $\Omega_{i',j'}$  that  $i' + j' = i_0 + j_0 + t + 1$ ,  $i' \geq i_0$ ,  $j' \geq j_0$ , we can divide the region  $\Omega_{i_0,i';j_0,j'}$  into four regions, namely  $\Omega_{i_0,i'-1;j_0,j'-1}$ ,  $\Omega_{i_0,i'-1;j',j'}$ ,  $\Omega_{i',i';j_0,j'-1}$  and  $\Omega_{i',j'}$ , apply a similar argument of  $2 \times 2$  subdomains as  $\Omega_{i_0,i_0+1;j_0,j_0+1}$ , and obtain that in  $\Omega_{i_0,i_0;j_0,j'}$

$$\begin{aligned} u_{i_0,i';j_0,j'} = & U_{i_0,i'-1;j_0,j'-1} \mu_{+1;i'-1}^{(1)} \mu_{+1;j'-1}^{(2)} + U_{i',i';j_0,j'-1} \mu_{-1;i'}^{(1)} \mu_{+1;j'-1}^{(2)} \\ & + U_{i_0,i'-1;j',j'} \mu_{+1;i'-1}^{(1)} \mu_{-1;j'}^{(2)} + u_{i',j'} \mu_{-1;j'}^{(1)} \mu_{-1;j'}^{(2)}, \end{aligned}$$

where  $U_{i_1,i_2;j_1,j_2} = \sum_{\substack{i_1 \leq i \leq i_2 \\ j_1 \leq j \leq j_2}} u_{i,j} \mu_{i,j}$ , thus we have (23). This completes the proof.  $\square$

The application of cardinal directional and corner directional trace transfers have been demonstrated in the construction of the subdomain solutions in the first sweep, and it is similar for the rest sweeps. However, we need to ensure that each subdomain problem is solved with the right transferred traces passed to it, thus next we focus on the movement of transferred traces, and have the following Lemma.

**Lemma 2.6.** *Suppose that  $\text{supp}(f) \subset \Omega_{i_0,j_0}$ , then DDM solution  $u_{DDM}$  of Algorithm 2.1 is indeed the solution to the problem  $P_\Omega$  in the constant medium case.*

The verification of the above Lemma is similar to the verification in [26] in the source transfer case, the main difference is that the case of trace transfer is simpler since the transferred traces have only cardinal directions while the transferred sources have all directions. Without loss of generality, a  $5 \times 5$  ( $N_1 = N_2 = 5$ ) domain partition and a source lying in  $\Omega_{3,3}$  ( $i_0 = j_0 = 3$ ) are used in the verification, and the movement of transferred traces in each sweep is checked as follows.

In the **first sweep** of direction  $(+1,+1)$ , the solution in the upper-right region  $\Omega_{i_0,N_1;j_0,N_2} = \Omega_{3,5;3,5}$  is to be constructed. The sweep contains  $N_1 + N_2 - 1 = 5 + 5 - 1 = 9$  steps, and the subdomain problems of  $\{\Omega_{i,j}\}$  with  $(i-1) + (j-1) + 1 = s$  in the region are solved at the  $s$ -th step of the sweep. The subdomain solutions are all zeros in the first  $(i_0-1) + (j_0-1) = 4$  steps since the local sources are all zeros. Then at the step  $(i_0-1) + (j_0-1) + 1 = 5$ , the subdomain problem of  $\Omega_{i_0,j_0} = \Omega_{3,3}$  is solved with the original source  $f = f_{3,3}$ , and four transferred source in cardinal directions are generated, as is shown in 4-(a). At step 6, the subdomain problems in  $\Omega_{4,3}$  and  $\Omega_{3,4}$  are solved, each of them takes one transferred trace from  $\Omega_{3,3}$ , and generates three new transferred traces, as shown in 4-(b). At step 7, the subdomain problems of  $\Omega_{5,3}$  and  $\Omega_{3,5}$  are solved similar to the previous step, while the subdomain problem of  $\Omega_{4,4}$  is solved with the transferred traces from  $\Omega_{3,4}$  and  $\Omega_{4,3}$ , and two new ones are generated, as shown in 4-(c). In the following steps, the subdomain problems are solved similarly, after  $N_1 + N_2 - 1 = 9$  steps the exact solution in the upper-right region is obtained.

In the **second sweep** of direction  $(-1,+1)$ , the solution in the upper-left region  $\Omega_{1,i_0-1;j_0,N_2} = \Omega_{1,2;3,5}$  is to be constructed, and the subdomain problems of  $\{\Omega_{i,j}\}$  in the region with  $(N_1 - i) + (j-1) + 1 = 5 - i + j = s$  are solved at the  $s$ -th step of the sweep. Among all the unused transferred traces from the previous sweep, the ones in the similar direction with current sweep are needed, while the others are not, as is shown in Figure 4-(d). The needed unused transferred traces is selected by the similar direction Rule 2.3, and it's obvious the opposite direction Rule 2.3 doesn't apply. The steps of the sweep are similar to the steps of the previous sweep, hence the details are omitted, the step 6 and 7 are shown in Figure 4-(e) and (f), after  $N_1 + N_2 - 1 = 9$  steps the exact solution in the upper-left region are obtained.

$\Omega_{1,5}$	$\Omega_{2,5}$	$\Omega_{3,5}$	$\Omega_{4,5}$	$\Omega_{5,5}$
$\Omega_{1,4}$	$\Omega_{2,4}$	$\Omega_{3,4}$	$\Omega_{4,4}$	$\Omega_{5,4}$
$\Omega_{1,3}$	$\Omega_{2,3}$	$\Omega_{3,3}$	$\Omega_{4,3}$	$\Omega_{5,3}$
$\Omega_{1,2}$	$\Omega_{2,2}$	$\Omega_{3,2}$	$\Omega_{4,2}$	$\Omega_{5,2}$
$\Omega_{1,1}$	$\Omega_{2,1}$	$\Omega_{3,1}$	$\Omega_{4,1}$	$\Omega_{5,1}$

(a) First sweep: step 5

$\Omega_{1,5}$	$\Omega_{2,5}$	$\Omega_{3,5}$	$\Omega_{4,5}$	$\Omega_{5,5}$
$\Omega_{1,4}$	$\Omega_{2,4}$	$\Omega_{3,4}$	$\Omega_{4,4}$	$\Omega_{5,4}$
$\Omega_{1,3}$	$\Omega_{2,3}$	$\Omega_{3,3}$	$\Omega_{4,3}$	$\Omega_{5,3}$
$\Omega_{1,2}$	$\Omega_{2,2}$	$\Omega_{3,2}$	$\Omega_{4,2}$	$\Omega_{5,2}$
$\Omega_{1,1}$	$\Omega_{2,1}$	$\Omega_{3,1}$	$\Omega_{4,1}$	$\Omega_{5,1}$

(b) First sweep: step 6

$\Omega_{1,5}$	$\Omega_{2,5}$	$\Omega_{3,5}$	$\Omega_{4,5}$	$\Omega_{5,5}$
$\Omega_{1,4}$	$\Omega_{2,4}$	$\Omega_{3,4}$	$\Omega_{4,4}$	$\Omega_{5,4}$
$\Omega_{1,3}$	$\Omega_{2,3}$	$\Omega_{3,3}$	$\Omega_{4,3}$	$\Omega_{5,3}$
$\Omega_{1,2}$	$\Omega_{2,2}$	$\Omega_{3,2}$	$\Omega_{4,2}$	$\Omega_{5,2}$
$\Omega_{1,1}$	$\Omega_{2,1}$	$\Omega_{3,1}$	$\Omega_{4,1}$	$\Omega_{5,1}$

(c) First sweep: step 7

$\Omega_{1,5}$	$\Omega_{2,5}$	$\Omega_{3,5}$	$\Omega_{4,5}$	$\Omega_{5,5}$
$\Omega_{1,4}$	$\Omega_{2,4}$	$\Omega_{3,4}$	$\Omega_{4,4}$	$\Omega_{5,4}$
$\Omega_{1,3}$	$\Omega_{2,3}$	$\Omega_{3,3}$	$\Omega_{4,3}$	$\Omega_{5,3}$
$\Omega_{1,2}$	$\Omega_{2,2}$	$\Omega_{3,2}$	$\Omega_{4,2}$	$\Omega_{5,2}$
$\Omega_{1,1}$	$\Omega_{2,1}$	$\Omega_{3,1}$	$\Omega_{4,1}$	$\Omega_{5,1}$

(d) After first sweep

$\Omega_{1,5}$	$\Omega_{2,5}$	$\Omega_{3,5}$	$\Omega_{4,5}$	$\Omega_{5,5}$
$\Omega_{1,4}$	$\Omega_{2,4}$	$\Omega_{3,4}$	$\Omega_{4,4}$	$\Omega_{5,4}$
$\Omega_{1,3}$	$\Omega_{2,3}$	$\Omega_{3,3}$	$\Omega_{4,3}$	$\Omega_{5,3}$
$\Omega_{1,2}$	$\Omega_{2,2}$	$\Omega_{3,2}$	$\Omega_{4,2}$	$\Omega_{5,2}$
$\Omega_{1,1}$	$\Omega_{2,1}$	$\Omega_{3,1}$	$\Omega_{4,1}$	$\Omega_{5,1}$

(e) Second sweep: step 6

$\Omega_{1,5}$	$\Omega_{2,5}$	$\Omega_{3,5}$	$\Omega_{4,5}$	$\Omega_{5,5}$
$\Omega_{1,4}$	$\Omega_{2,4}$	$\Omega_{3,4}$	$\Omega_{4,4}$	$\Omega_{5,4}$
$\Omega_{1,3}$	$\Omega_{2,3}$	$\Omega_{3,3}$	$\Omega_{4,3}$	$\Omega_{5,3}$
$\Omega_{1,2}$	$\Omega_{2,2}$	$\Omega_{3,2}$	$\Omega_{4,2}$	$\Omega_{5,2}$
$\Omega_{1,1}$	$\Omega_{2,1}$	$\Omega_{3,1}$	$\Omega_{4,1}$	$\Omega_{5,1}$

(f) Second sweep: step 7

Figure 4: The first sweep  $(+1, +1)$  and the second sweep  $(-1, +1)$  of the diagonal sweeping DDM in  $\mathbb{R}^2$  with trace transfer. The source is supported in  $\Omega_{3,3}$ . The arrows denote the transferred traces with their directions, the red ones are in the similar direction of the current sweep, while the green ones are not, thus only the red ones are used in the current sweep due to similar direction Rule 2.3.

In the **third sweep** of direction  $(+1, -1)$ , the solution in the lower-right region  $\Omega_{i_0, N_1; 1, j_0-1} = \Omega_{3,5; 1,2}$  is to be constructed. Among all the unused transferred traces from the previous sweeps, the ones from the upper-right region are needed, while the ones from the upper-left region are not, as is shown in Figure 5-(a). The unused transferred traces from the upper right region are selected since they stratify both the Rule 2.3 and 2.4, on the other hand, the unused transferred traces from the upper left region are excluded by the opposite direction Rule 2.4, since they are from the second sweep which is in the opposite direction of the current sweep. The steps of the sweep are similar to the steps of previous sweeps, and the step 6 and 7 are shown in Figure 5-(b) and (c), after  $N_1 + N_2 - 1 = 9$  steps the exact solution in the lower-right region is obtained.

In the **fourth sweep** of direction  $(-1, -1)$ , the solution in the lower-left region  $\Omega_{1, i_0-1; 1, j_0-1} = \Omega_{1,2; 1,2}$  is to be constructed. All the unused transferred traces from the previous sweeps are needed, as is shown in Figure 5-(d). They are all selected by the similar direction Rule 2.3, and since they are not from the opposite sweep, i.e., the first sweep, the opposite direction Rule 2.4 does not apply to them. The steps of the sweep are similar to the steps of the previous sweeps, and the step 7 of the sweep are shown in Figure 5-(e), and finally after  $N_1 + N_2 - 1 = 9$  steps, the exact solution in

$\Omega_{1,5}$	$\Omega_{2,5}$	$\Omega_{3,5}$	$\Omega_{4,5}$	$\Omega_{5,5}$
$\Omega_{1,4}$	$\Omega_{2,4}$	$\Omega_{3,4}$	$\Omega_{4,4}$	$\Omega_{5,4}$
$\Omega_{1,3}$	$\Omega_{2,3}$	$\Omega_{3,3}$	$\Omega_{4,3}$	$\Omega_{5,3}$
$\downarrow$ $\Omega_{1,2}$	$\Omega_{2,2}$	$\Omega_{3,2}$	$\Omega_{4,2}$	$\Omega_{5,2}$
$\Omega_{1,1}$	$\Omega_{2,1}$	$\Omega_{3,1}$	$\Omega_{4,1}$	$\Omega_{5,1}$

(a) Before third sweep

$\Omega_{1,5}$	$\Omega_{2,5}$	$\Omega_{3,5}$	$\Omega_{4,5}$	$\Omega_{5,5}$
$\Omega_{1,4}$	$\Omega_{2,4}$	$\Omega_{3,4}$	$\Omega_{4,4}$	$\Omega_{5,4}$
$\Omega_{1,3}$	$\Omega_{2,3}$	$\Omega_{3,3}$	$\Omega_{4,3}$	$\Omega_{5,3}$
$\downarrow$ $\Omega_{1,2}$	$\Omega_{2,2}$	$\Omega_{3,2}$	$\Omega_{4,2}$	$\Omega_{5,2}$
$\Omega_{1,1}$	$\Omega_{2,1}$	$\Omega_{3,1}$	$\Omega_{4,1}$	$\Omega_{5,1}$

(b) Third sweep: step 6

$\Omega_{1,5}$	$\Omega_{2,5}$	$\Omega_{3,5}$	$\Omega_{4,5}$	$\Omega_{5,5}$
$\Omega_{1,4}$	$\Omega_{2,4}$	$\Omega_{3,4}$	$\Omega_{4,4}$	$\Omega_{5,4}$
$\Omega_{1,3}$	$\Omega_{2,3}$	$\Omega_{3,3}$	$\Omega_{4,3}$	$\Omega_{5,3}$
$\downarrow$ $\Omega_{1,2}$	$\Omega_{2,2}$	$\Omega_{3,2}$	$\Omega_{4,2}$	$\Omega_{5,2}$
$\Omega_{1,1}$	$\Omega_{2,1}$	$\Omega_{3,1}$	$\Omega_{4,1}$	$\Omega_{5,1}$

(c) Third sweep: step 7

$\Omega_{1,5}$	$\Omega_{2,5}$	$\Omega_{3,5}$	$\Omega_{4,5}$	$\Omega_{5,5}$
$\Omega_{1,4}$	$\Omega_{2,4}$	$\Omega_{3,4}$	$\Omega_{4,4}$	$\Omega_{5,4}$
$\Omega_{1,3}$	$\Omega_{2,3}$	$\Omega_{3,3}$	$\Omega_{4,3}$	$\Omega_{5,3}$
$\downarrow$ $\Omega_{1,2}$	$\Omega_{2,2}$	$\Omega_{3,2}$	$\Omega_{4,2}$	$\Omega_{5,2}$
$\Omega_{1,1}$	$\Omega_{2,1}$	$\Omega_{3,1}$	$\Omega_{4,1}$	$\Omega_{5,1}$

(d) After third sweep

$\Omega_{1,5}$	$\Omega_{2,5}$	$\Omega_{3,5}$	$\Omega_{4,5}$	$\Omega_{5,5}$
$\Omega_{1,4}$	$\Omega_{2,4}$	$\Omega_{3,4}$	$\Omega_{4,4}$	$\Omega_{5,4}$
$\Omega_{1,3}$	$\Omega_{2,3}$	$\Omega_{3,3}$	$\Omega_{4,3}$	$\Omega_{5,3}$
$\downarrow$ $\Omega_{1,2}$	$\Omega_{2,2}$	$\Omega_{3,2}$	$\Omega_{4,2}$	$\Omega_{5,2}$
$\Omega_{1,1}$	$\Omega_{2,1}$	$\Omega_{3,1}$	$\Omega_{4,1}$	$\Omega_{5,1}$

(e) Fourth sweep: step 7

$\Omega_{1,5}$	$\Omega_{2,5}$	$\Omega_{3,5}$	$\Omega_{4,5}$	$\Omega_{5,5}$
$\Omega_{1,4}$	$\Omega_{2,4}$	$\Omega_{3,4}$	$\Omega_{4,4}$	$\Omega_{5,4}$
$\Omega_{1,3}$	$\Omega_{2,3}$	$\Omega_{3,3}$	$\Omega_{4,3}$	$\Omega_{5,3}$
$\Omega_{1,2}$	$\Omega_{2,2}$	$\Omega_{3,2}$	$\Omega_{4,2}$	$\Omega_{5,2}$
$\Omega_{1,1}$	$\Omega_{2,1}$	$\Omega_{3,1}$	$\Omega_{4,1}$	$\Omega_{5,1}$

(f) After fourth sweep

Figure 5: The third sweep (+1, -1) and the fourth sweep (-1, -1) of the diagonal sweeping DDM in  $\mathbb{R}^2$  with trace transfer. The source is supported in  $\Omega_{3,3}$ . The arrows denote the transferred traces with their directions, the red ones are in the similar direction to the current sweep and not against the opposite direction Rule 2.3, the green ones are in the similar direction but against the opposite direction Rule 2.3, and the blue ones are not in the similar direction, thus only the red ones are used in the current sweep.

the total region is obtained, as is shown in Figure 5-(f).

For the case of general  $f$ , clearly  $u(f) = \sum_{i,j} u(f_{i,j})$ , where  $u(g)$  denotes the solution to the problem  $\mathcal{P}_\Omega$  with the source  $g$ , therefore we have the following theorem by Lemma 2.6,

**Theorem 2.7.** *The DDM solution  $u_{DDM}$  of Algorithm 2.1 is the solution to the problem  $\mathcal{P}_\Omega$  in the constant medium case.*

The above theorem general no longer holds in the inhomogeneous case, however, in the two-layered medium case and under certain conditions, the exactness of the DDM solution can still be achieved, which is discussed in the next section.

### 3. The diagonal sweeping DDM with trace transfer in $\mathbb{R}^2$ in the two-layered medium case

The layered medium problem is one of the basic problems in many applications involving the Helmholtz equation, for example, in seismology, the seismic wave traveling in the layered structure is extensively studied for imaging the earth interior. The diagonal sweeping DDM handles the layered medium in a proper way that, by average, the forward sweep for the incident and the backward sweep for the reflection is accomplished in one iteration for the multilayered medium problem, while the L-sweep method [32] only deals the forward sweep for the incident in one iteration. Such property of the diagonal sweeping DDM has been studied numerically in [26], here the DDM solution is analyzed in detail in the two-layered medium case. Suppose the medium has an interface  $x_2 = \eta_L$ , so that the wave number  $k$  satisfies that

$$k = \begin{cases} k_2, & x_2 > \eta_L, \\ k_1, & x_2 \leq \eta_L, \end{cases} \quad (27)$$

as is demonstrated in Figure 6 (left). The well-posedness and convergence of such a PML problem with two-layered medium have been proved in [6]. In this section, the case of  $1 \times 2$  partition is first discussed for sweeping type DDM to establish some basic properties of the trace transfer in layered medium case, then the case of general partition is considered.

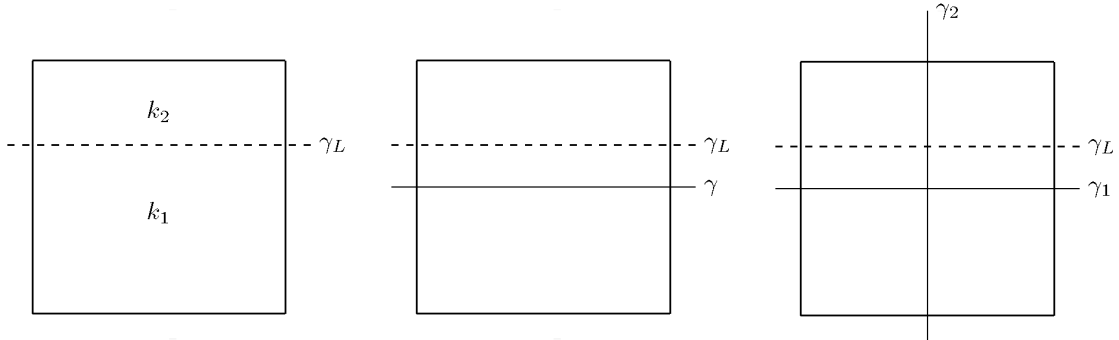


Figure 6: Two-layered medium problem (left) and its  $1 \times 2$  (middle) or  $2 \times 2$  (right) domain decomposition.

#### 3.1. Two subdomains

The sweeping DDM with trace transfer with two subdomains uses one forward sweep and one backward sweep, which is stated below. Suppose the domain  $\Omega = (-l_1, l_1) \times (-l_2, l_2)$  is partitioned into two subdomains  $\Omega_1 = (-l_1, l_1) \times (-l_2, 0)$  and  $\Omega_2 = (-l_1, l_1) \times (0, l_2)$ , by the  $x$  axis, which is denoted by  $\gamma$ , as is shown in Figure 6 (middle). The upper half-plane is defined as  $\Omega^+ = \{(x_1, x_2) | x_2 > 0\}$ , and the lower half-plane  $\Omega^- = \{(x_1, x_2) | x_2 < 0\}$ . We denote  $G_1$  and  $G_2$  the fundamental solution to problem  $\mathcal{P}_{\Omega_1}$  and  $\mathcal{P}_{\Omega_2}$ , respectively. The potential associated with the subdomain  $\Omega_1$  and  $\Omega_2$  are defined by

$$\Psi_i(\lambda)(x) = \int_{\gamma} J_{\Omega_i}^{-1} G_i(x, y) \left( A_{\Omega_i} \nabla_y \lambda(y) \cdot \mathbf{n}_i \right) - \lambda(y) \left( A_{\Omega_i} \nabla_y (J_{\Omega_i}^{-1} G_i(x, y)) \cdot \mathbf{n}_i \right) dy,$$

where  $i = 1, 2$ ,  $\mathbf{n}_1 = (0, -1)$  and  $\mathbf{n}_2 = (0, +1)$ .

In the **first sweep** of upward direction, at step 1, the subdomain problem of  $\Omega_1$  is solved with the source  $f \cdot \chi_{\Omega_1}$ , and the solution is denoted  $u_1$ . Then at step 2, subdomain problem of  $\Omega_2$  is solved with the transferred trace in addition to the source  $f \cdot \chi_{\Omega_1}$ , and the solution is denoted  $u_2$ , which is given by

$$u_2 = \mathcal{L}_{\Omega_2}^{-1}(f \cdot \chi_{\Omega_2}) + \Psi_2(u_1). \quad (28)$$

In the **second sweep** of downward direction, the subdomain solution is zero at the step 1, and at the step 2, the subdomain problem of  $\Omega_1$  is solved with the transferred trace from  $\Omega_2$ , and the solution is denoted  $u'_1$ , which is given by

$$u'_1 = \Psi_1(u_2). \quad (29)$$

After the upward and downward sweep, the DDM solution is formed as

$$u_{\text{DDM}} = (u_1 + u'_1)\mu_{\Omega^-} + u_2\mu_{\Omega^+}. \quad (30)$$

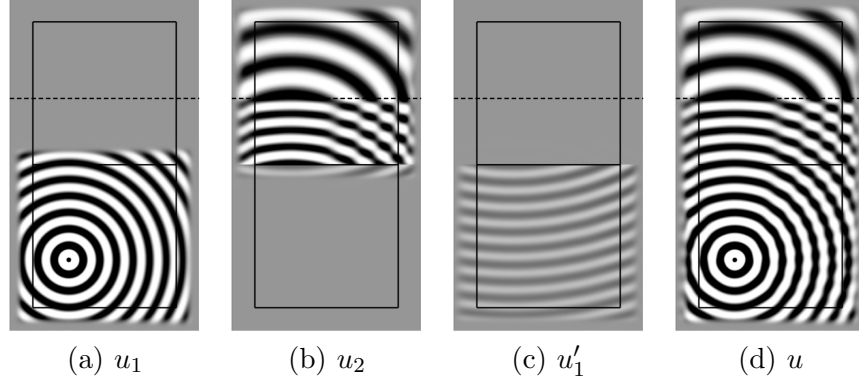


Figure 7: Illustration of sweeping DDM in two-layered medium case in  $\mathbb{R}^2$  with  $1 \times 2$  partition.

The DDM solution steps are demonstrated in Figure 7 in the case that  $\eta_L > \eta_2$  and  $f$  lies in  $\Omega_1$ , the subdomain solution  $u_1$  contains the up going wave of  $\Omega^-$ , the subdomain solution  $u_2$  is already exact in  $\Omega^+$ , and the subdomain solution  $u'_1$  contains the reflection in  $\Omega^-$  from  $\Omega^+$ , as are shown in Figure 7 (a)-(c), respectively. We have the following Lemma,

**Lemma 3.1.** *For smooth source  $f$ , the sweeping DDM solution (30) is the solution to  $\mathcal{P}_\Omega$  with source  $f$  in the two-layered medium case.*

*Proof.* In the case that the medium interface coincides with the subdomain interface, i.e.,  $\eta_L = \eta_2$ , it is obvious that the DDM solution (30) is exact due to the wave number definition (15) and Lemma 2.1. Thus we suppose that  $\eta_L > \eta_2$ , it is easy to see that the lemma also holds in the case that  $\text{supp } f \subset \Omega_2$ , therefore we only consider the case that  $\text{supp } f \subset \Omega_1$ .

Some notations are introduced first as follows. The solution to the problem  $\mathcal{P}_\Omega$  of wave number  $k$  with source  $f$  is denoted by  $u$ . Define the following two PML problems which are associated with  $\Omega$ ,  $\mathcal{P}_\Omega^k$  is the PML problem with two-layered medium  $k(x)$ , while  $\mathcal{P}_\Omega^{k_1}$  is the PML problem with

constant medium  $k_1$ . Let  $G^k$  and  $G^{k_1}$  be the fundamental solutions to  $\mathcal{P}_\Omega^k$  and  $\mathcal{P}_\Omega^{k_1}$ , respectively. Then define the potential associated with  $\mathcal{P}_\Omega^k$  as,

$$\Psi_\pm^k(\lambda)(x) = \int_\gamma J_k^{-1} G^k(x, y) \left( A^k \nabla \lambda(y) \cdot \mathbf{n}_\pm \right) - \lambda(y) \left( A^k \nabla (J_k^{-1} G^k(x, y)) \cdot \mathbf{n}_\pm \right) dy, \quad (31)$$

where  $n_\pm = (0, \pm 1)$ . The potential  $\Psi_\pm^{k_1}$  associated with  $\mathcal{P}_\Omega^{k_1}$  is defined similarly.

First we prove that the sweeping DDM solution is exact in the upper half-plane, that is,

$$u_2 = u, \quad \text{in } \Omega^+. \quad (32)$$

To prove this, we start by consider the case  $f$  is a delta function  $\delta(x - x')$ , where  $x' \in \Omega_1$ . In this case, the subdomain solution of  $\Omega_1$  at step 1 is  $G^{k_1}(x, x')$  in  $\Omega^-$ , and denoted  $G_{x'}^{k_1}$  for short. Then at step 2, the subdomain solution of  $\Omega_2$  is  $\Psi_2(G_{x'}^{k_1})$ . In the upper plane  $\Omega^+$ , by the property of uPML, we have that for any  $x'' \in \Omega^+$  and  $y \in \gamma$ ,  $G_2(x'', y) = G^k(x'', y)$ , thus  $\Psi_2(G_{x'}^{k_1}) = \Psi_+^k(G_{x'}^{k_1})$ . Then by (31) and (6) we have that for any  $x'' \in \Omega^+$ ,

$$\begin{aligned} & \Psi_+^k(G_{x'}^{k_1})(x'') \\ &= \int_\gamma J_k^{-1}(y) G^k(x'', y) \left( A_k \nabla G^{k_1}(y, x') \cdot \mathbf{n}_+ \right) \\ & \quad - G^{k_1}(y, x') \left( A_k \nabla (J_k^{-1}(y) G^k(x'', y)) \cdot \mathbf{n}_+ \right) dy \\ &= \frac{J_{k_1}(x')}{J_k(x'')} \int_\gamma J_{k_1}^{-1}(y) G^{k_1}(x', y) \left( A_{k_1} \nabla G^k(y, x'') \cdot \mathbf{n}_- \right) \\ & \quad - G^k(y, x'') \left( A_{k_1} \nabla (J_{k_1}^{-1}(y) G^{k_1}(x', y)) \cdot \mathbf{n}_- \right) dy \\ &= \frac{J_{k_1}(x')}{J_k(x'')} \Psi_-^{k_1}(G_{x''}^k)(x'), \end{aligned} \quad (33)$$

where  $G_{x''}^k$  is the fundamental solution to problem  $\mathcal{P}_\Omega^k$  with delta source  $\delta(x - x'')$ . Moreover, using the source transfer argument, we obtain that  $\Psi_-^{k_1}(G_{x''}^k)(x') = \Psi_-^k(G_{x''}^k)(x')$ , and by Lemma 2.1,  $\Psi_-^k(G_{x''}^k)(x') = G_{x''}^k(x')$ . Therefore, with the fact that  $J_{k_1}(x') = J_k(x')$ , (33) implies that for any  $x'' \in \Omega^+$ ,

$$\Psi_+^k(G_{x'}^{k_1})(x'') = \frac{J_{k_1}(x')}{J_k(x'')} G_{x''}^k(x') = G_{x'}^k(x''). \quad (34)$$

This indicates that (32) holds in the case  $f$  is a delta function  $\delta(x - x')$  in  $\Omega_1$ .

Now for general smooth  $f$  in  $\Omega_1$ , one can show that by Fubini's theorem, for any  $y \in \gamma$ ,

$$\begin{aligned} \nabla_y u_1(y) &= \nabla_y \int_{\Omega_1} f(x') G^{k_1}(y, x') dx' \\ &= \int_{\Omega_1} f(x') \nabla_y G^{k_1}(y, x') dx'. \end{aligned} \quad (35)$$

Then by (34) and (35), we can show that for any  $x'' \in \Omega^+$ ,

$$\begin{aligned}
u_2(x'') &= \Psi_+^k(u_1)(x'') \\
&= \int_{\gamma} J_k^{-1}(y) G^k(x'', y) \left( A^k(y) \nabla_y u_1(y) \cdot \mathbf{n}_2 \right) - u_1(y) \left( A^k(y) \nabla_y (J_k^{-1}(y) G^k(x, y)) \cdot \mathbf{n}_2 \right) dy \\
&= \int_{\gamma} \left( J_k^{-1}(y) G^k(x'', y) \left( A^k(y) \int_{\Omega_1} f(x') \nabla_y G^{k_1}(y, x') dx' \cdot \mathbf{n}_2 \right) \right. \\
&\quad \left. - \left( \int_{\Omega_1} f(x') G^{k_1}(y, x') dx' \right) \left( A^k(y) \nabla_y (J_k^{-1}(y) G^k(x'', y)) \cdot \mathbf{n}_2 \right) \right) dy. \tag{36}
\end{aligned}$$

The fundamental solution  $G^{k_1}$ ,  $G^k$  and their derivatives are singular at  $x = x'$ , but still integrable on  $\Omega_1$ , furthermore, they decay exponentially outside of  $\Omega_1$ , consequently, the order of integration in (36) can be changed by Fubini's theorem, therefore we can show that for any  $x'' \in \Omega^+$ ,

$$\begin{aligned}
u_2(x'') &= \int_{\Omega_1} f(x') dx' \left( \int_{\gamma} J_k^{-1}(y) G^k(x'', y) \left( A^k(y) \nabla_y G^{k_1}(y, x') \cdot \mathbf{n}_2 \right) \right. \\
&\quad \left. - G^{k_1}(y, x') \left( A^k(y) \nabla_y (J_k^{-1}(y) G^k(x'', y)) \cdot \mathbf{n}_2 \right) dy \right) \\
&= \int_{\Omega_1} f(x') G_{x'}^k(x'') dx' \\
&= u(x'').
\end{aligned}$$

Having proved that the sweeping DDM solution is exact in the upper half-plane  $\Omega^+$ , next we prove that it is also exact in the lower half-plane  $\Omega^-$ , that is,

$$u_1 + u'_1 = u, \quad \text{in } \Omega^-. \tag{37}$$

From (29) we know the limit value of subdomain solution  $u_2 = \Psi_2(u_1)$  on  $\gamma$  from the  $\Omega^-$  side is needed to evaluate  $u'_1$ .

Since the medium interface is away from the subdomain interface, where the distance is denoted  $d_k$ , we can introduce a smooth cutoff function  $\beta_k(x_2) = \beta(\frac{x_2 - d_k}{d_k/2})$ , which is nonzero only in the region  $(-\infty, \infty) \times (d_k/2, d_k)$ , denoted by  $\Omega_\beta$ . Let

$$v = (u - u_1)\beta_k, \quad \text{in } \mathbb{R}^2, \tag{38}$$

and it is clear that

$$\mathcal{L}^k v = 0 \quad \text{in } \mathbb{R}^2 / \Omega_\beta. \tag{39}$$

This indicates that  $v$  is the solution to the problem  $\mathcal{P}^k$  with the source lying in  $\Omega_\beta$ . Let  $\tilde{v}$  be the solution to the problem  $\mathcal{P}_{\Omega_2}$  of wave number  $k$  with the same source, that is,

$$\mathcal{L}_{\Omega_2} \tilde{v} = \mathcal{L}^k v, \quad \text{in } \mathbb{R}^2, \tag{40}$$

which implies using Lemma 2.1 that,

$$\Psi_2(\tilde{v}) = -\tilde{v}, \quad \text{in } \Omega^-. \tag{41}$$

Besides, since the problem  $\mathcal{P}_{\Omega_2}$  is a subdomain problem of  $\mathcal{P}_{\Omega}^k$ , while  $v$  and  $\tilde{v}$  shares the same source, we know that  $v = \tilde{v}$  on  $\gamma$ , this imples by (38) and (41) that,

$$\Psi_2(u - u_1) = -\tilde{v}, \quad \text{in } \Omega^-.$$

By Lemma 2.2,  $\Psi_2(u) = 0$  in  $\Omega^-$ , consequently,

$$\Psi_2(u_1) = \tilde{v}, \quad \text{in } \Omega^-. \quad (42)$$

Therefore we know that

$$\lim_{x_2 \rightarrow 0^-} u_2 = u - u_1. \quad (43)$$

On the other hand,  $v$  also satisfies that

$$\mathcal{L}^{k_1} v = 0 \quad \text{in } \mathbb{R}^2 / \Omega_{\beta}, \quad (44)$$

thus using Lemma 2.1 we have that

$$\Psi_1(v) = \Psi_-^{k_1}(v) = v, \quad \text{in } \Omega^-, \quad (45)$$

this shows by (38), (43) that

$$\Psi_1(u_2) = u - u_1, \quad \text{in } \Omega^-, \quad (46)$$

and (37) is porved. This completes the proof.  $\square$

### 3.2. General partition

For the general checkerboard partition of  $N_1 \times N_2$ , the solution of the diagonal sweeping DDM with trace transfer is exactly the solution to  $\mathcal{P}_{\Omega}$  in the two-layered medium case, provided the source and the first swept subdomain are on the same side of the medium interface. For example, with the sweeping order of Algorithm 2.1, the DDM solution is exact if the source is supported below the medium interface. In the case the source is above the medium interface, one more iteration is needed to construct the exact solution. Without loss of generality, the  $2 \times 2$  partition case is considered for demonstration. Again, the solution of diagonal sweeping DDM is exact in the case that the medium interface coincides with the subdomain interface, i.e.,  $\eta_L = \eta_2$ , the proof is quite similar to the case of constant medium and thus omitted. Then we assume that the  $\eta_L > \eta_2$ , and since the cases that the source lies in one of the four subdomains while below the medium interface are similar, here we suppose the source lies in  $\Omega_{1,1}$ .

For simplicity, the following notations are used for the  $2 \times 2$  partition of the domain  $\Omega = (-l_1, l_1) \times (-l_2, l_2)$ . Let  $\Omega_1^-$  and  $\Omega_1^+$  be the left and right half-plane, while  $\Omega_2^-$  and  $\Omega_2^+$  be the lower and upper half-plane, respectively. The characteristic functions for half-planes are defined as  $\chi_i^{\pm} = \chi_{\Omega_i^{\pm}}$ ,  $i = 1, 2$ . The four quadrants are denoted as  $\Omega^{+;+}$ ,  $\Omega^{-;+}$ ,  $\Omega^{-;-}$  and  $\Omega^{+;-}$ , and the  $x$  and  $y$  axes are denoted  $\gamma_1$  and  $\gamma_2$ , respectively, as is shown in Figure 6 (right).

It is clear that the problem  $\mathcal{P}_{\Omega_{1,1;1,2}}$  of the *left* half region is a two-layered medium problem using  $1 \times 2$  partition, of which the solution to source  $f$  is denoted  $u_{Lf}$ , as is shown in Figure 8 (a). On the other hand, taking the region  $\Omega_{1,2;1,1}$  and  $\Omega_{1,2;2,2}$  as two subdomains, the problem  $\mathcal{P}_{\Omega}$  is also a two-layered medium problem using  $1 \times 2$  partition, of which the lower subdomain solution

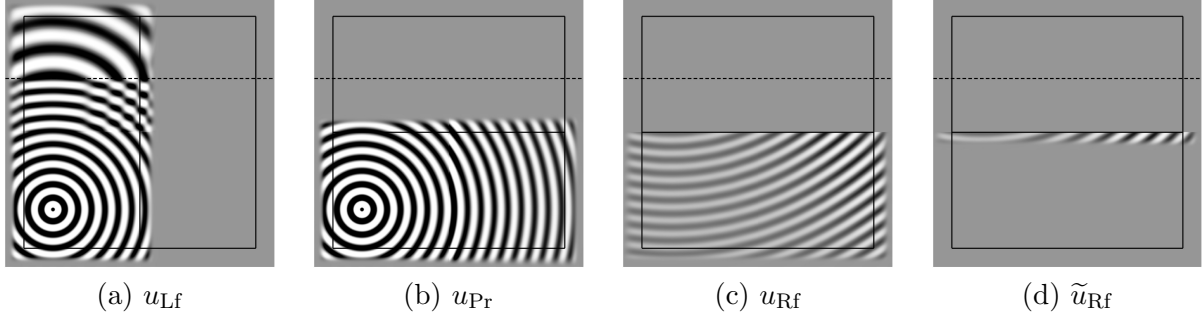


Figure 8: Illustration of partial solutions of diagonal sweeping DDM in the two-layered medium case in  $\mathbb{R}^2$  with  $2 \times 2$  partition.

in the first sweep is the *prediction* of the total solution with constant medium, thus is denoted  $u_{Pr}$  (shown in Figure 8 (b)). The lower subdomain solution in the second sweep is the *reflection* from medium interface, thus is denoted  $u_{Rf}$  (shown in Figure 8 (c)). Since the reflection in lower subdomain is caused by the medium change in the upper subdomain, or equivalently, caused by a source in the upper subdomain, we can define the PML solution of the reflection for the upper subdomain problem as  $\tilde{u}_{Rf}$ , which is illustrated in Figure 8 (d), which satisfies  $u_{Rf} = \tilde{u}_{Rf}$  on  $\gamma_1$  and  $\tilde{u}_{Rf}$  decays exponentially in the lower half-plane.

In the **first sweep** of direction  $(+1, +1)$ , at step 1, the subdomain problem of  $\Omega_{1,1}$  is solved with the source  $f$ , the solution  $u_{1,1}^1$  is obtained, as is shown in Figure 9 (a). At step 2, the subdomain problem in  $\Omega_{2,1}$  is solved with the transferred trace from  $\Omega_{1,1}$ , the solution  $u_{2,1}^1$  is obtained, as is shown in Figure 9 (b), and by applying  $x$ -directional trace transfer on  $\Omega_{1,2;1,1}$ , we can show that

$$u_{2,1}^1 = \begin{cases} u_{Pr}, & \text{in } \Omega^{+;-} \\ 0, & \text{in } \Omega^{-;-} \end{cases} \quad (47)$$

thus one upward transferred traces are generated from  $\Omega_{2,1}$ . In addition, the subdomain problem in  $\Omega_{1,2}$  is solved with the transferred trace from  $\Omega_{1,1}$ , the solution  $u_{1,2}^1$  is obtained, as is shown in Figure 9 (c), and by applying  $y$ -directional trace transfer for two-layered medium on  $\Omega_{1,1;1,2}$ , we can show that

$$u_{1,2}^1 = \begin{cases} u, & \text{in } \Omega^{-;+} \\ \tilde{u}_{Rf}, & \text{in } \Omega^{-;-} \end{cases} \quad (48)$$

This shows that two transferred traces are generated from  $\Omega_{1,2}$ , one is rightwards, and one is downwards.

At step 3, the subdomain problem in  $\Omega_{2,2}$  is solved with the transferred trace from  $\Omega_{1,2}$  and  $\Omega_{2,1}$ , the solution  $u_{2,2}^1$  is obtained, as is shown in Figure 9 (d), and we will show that  $u_{2,2}^1 = u$  in  $\Omega_{2,2}$ . By (47) and (48), it is easy to see that

$$\begin{aligned} u_{2,2}^1 &= \Phi_{-1,0;2,2}(u_{1,2}^1) + \Phi_{0,-1;2,2}(u_{2,1}^1) \\ &= \Phi_{-1,0;2,2}(u\chi_2^+ + \tilde{u}_{Rf}\chi_2^-) + \Phi_{0,-1;2,2}(u_{Pr}\chi_1^+) \\ &= \left( \Phi_{-1,0;2,2}(u\chi_2^+) + \Phi_{0,-1;2,2}(u\chi_1^+) \right) \\ &\quad + \left( \Phi_{-1,0;2,2}(\tilde{u}_{Rf}\chi_2^-) - \Phi_{0,-1;2,2}((u - u_{Pr})\chi_1^+) \right). \end{aligned} \quad (49)$$

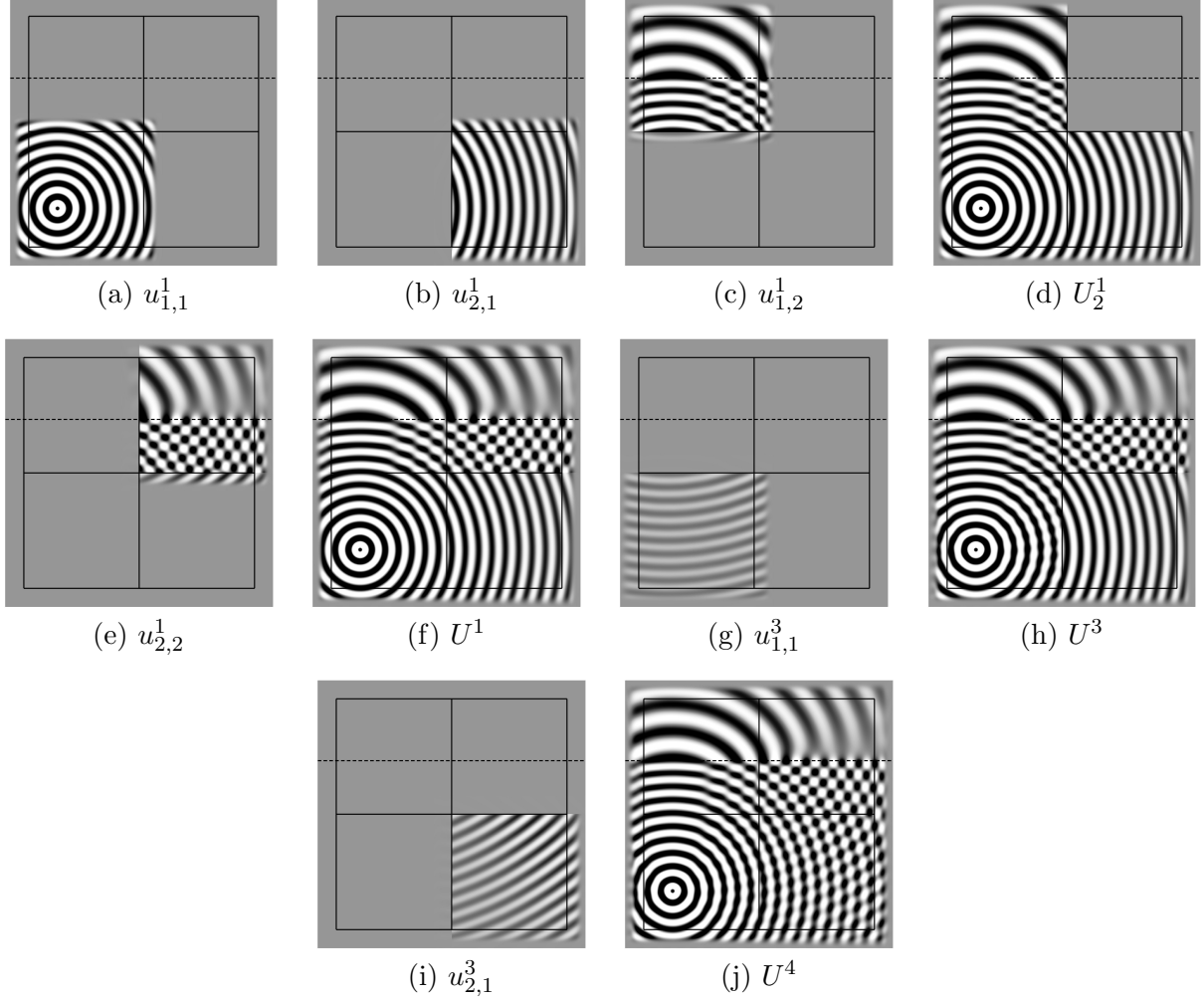


Figure 9: Illustration of diagonal sweeping DDM with trace transfer in the two-layered medium case in  $\mathbb{R}^2$  with  $2 \times 2$  partition.  $U^{(l)}$ ,  $l = 1, 2, 3, 4$  denotes the DDM solution after sweep  $l$ , and  $U_i^{(l)}$  denotes the DDM solution at  $i$ -th step of sweep  $l$ .

Applying corner direction trace transfer on  $\Omega_{2,2}$ , for the first term of RHS of (49), we have that

$$\Phi_{-1,0;2,2}(u\chi_2^+) + \Phi_{0,-1;2,2}(u\chi_1^+) = u\chi_1^+\chi_2^+, \quad (50)$$

Moreover, we can show that for the second term in RHS of (49)

$$\Phi_{-1,0;2,2}(\tilde{u}_{\text{Rf}}\chi_2^-) - \Phi_{0,-1;2,2}((u - u_{\text{Pr}})\chi_1^+) = \tilde{u}_{\text{Rf}}\chi_1^+\chi_2^-, \quad (51)$$

where we have used the fact that  $u_{\text{Rf}} + u_{\text{Pr}} = u$  on  $\gamma_1$ , and the corner directional trace transfer on  $\Omega_{2,1}$ . Therefore,

$$u_{2,2}^1 = u\chi_1^+\chi_2^+ + \tilde{u}_{\text{Rf}}\chi_1^+\chi_2^-, \quad (52)$$

which implies that the exact solution in  $\Omega_{2,2}$  is obtained, as is shown in Figure 9 (e), and a downward transferred trace is generated on  $\gamma_1$ . After the first sweep, the subdomain solutions in  $\Omega_{1,2}$  and  $\Omega_{2,2}$

are exact, while the reflection waves are missing in the subdomain solutions in  $\Omega_{1,1}$  and  $\Omega_{2,1}$ , as is shown in Figure 9 (f). Besides, two downwards transferred traces from  $\Omega_{1,2}$  and  $\Omega_{2,2}$  are generated and will be used in the following sweeps.

All the subdomain sources and solutions are zero in the **second sweep** of direction  $(+1, -1)$ , since the two transferred traces are not used in the sweep due to the similar direction rule. In the **third sweep** of  $(-1, +1)$ , the subdomain solution is zero in step 1. Then at step 2, the subdomain problem of  $\Omega_{1,1}$  with the transferred trace from  $\Omega_{1,2}$  is solved, and the solution  $u_{1,1}^3$  is obtained. By the argument of the two-layered subdomains, we obtain that

$$u_{1,1}^3 = \begin{cases} u_{\text{Rf}}, & \text{in } \Omega^{-;+} \\ 0, & \text{in } \Omega_2^+ \end{cases}, \quad (53)$$

as is shown in Figure 9 (g). This implies that the missing reflections in  $\Omega_{1,1}$  is recovered, as is shown in Figure 9 (h), and a rightward transferred trace is generated. At step 3, the subdomain problem in  $\Omega_{2,1}$  with the transferred traces from  $\Omega_{1,1}$  and  $\Omega_{2,2}$  is solved, and the solution  $u_{2,1}^3$  is obtained. By (52) and (53), we know that

$$\begin{aligned} u_{2,1}^3 &= \Phi_{-1,0;2,1}(u_{1,1}^3) + \Phi_{0,+1;2,1}(u_{2,2}^1) \\ &= \Phi_{-1,0;2,1}(u_{\text{Rf}}\chi_2^-) + \Phi_{0,+1;2,1}(u_{\text{Rf}}\chi_1^+) \end{aligned} \quad (54)$$

$$= u_{\text{Rf}}\chi_1^+ \chi_2^-, \quad (55)$$

thus the missing reflection in  $\Omega_{2,1}$  is obtained, as is shown in Figure 9 (i), and no more transferred traces are generated. All subdomain solutions in the **final sweep** are zero, and at last the total exact solution is constructed in  $\Omega$ , as is shown in Figure 9 (j). Thus the verification of the exactness of the solution is finished.

#### 4. The diagonal sweeping DDM with trace transfer in $\mathbb{R}^3$

In this section, the diagonal sweeping DDM with trace transfer in  $\mathbb{R}^2$  is extended to  $\mathbb{R}^3$ . The PML equation in  $\mathbb{R}^3$  for the cuboidal box  $B = \{(x_1, x_2, x_3)^T : a_j \leq x_j \leq b_j, j = 1, 2, 3\}$  could be defined as

$$J_B^{-1} \nabla \cdot (A_B \nabla \tilde{u}) + k^2 \tilde{u} = f, \quad \text{in } \mathbb{R}^3, \quad (56)$$

with

$$A_B(x) = \text{diag} \left( \frac{\alpha_2(x_2)\alpha_3(x_3)}{\alpha_1(x_1)}, \frac{\alpha_1(x_1)\alpha_3(x_3)}{\alpha_2(x_2)}, \frac{\alpha_1(x_1)\alpha_2(x_2)}{\alpha_3(x_3)} \right), \quad J_B(x) = \alpha_1(x_1)\alpha_2(x_2)\alpha_3(x_3),$$

where  $\alpha_3(x_3) = 1 + i\sigma_3(x_3)$  and  $\sigma_3(x_3)$  is defined in the same way as (3).

With the  $z$ -direction partition as  $\zeta_k = -l_3 + (k - 1)\Delta\zeta$  for  $k = 1, \dots, N_3 + 1$ , where  $\Delta\zeta = 2l_3/N_3$ , the cuboidal domain  $\Omega = (-l_1, l_1) \times (-l_2, l_2) \times (-l_3, l_3)$  in  $\mathbb{R}^3$  is partitioned into  $N_1 \times N_2 \times N_3$  nonoverlapping subdomains  $\Omega_{i,j,k}$ , and the source is decomposed into  $f_{i,j,k} = f \cdot \chi_{\Omega_{i,j,k}}$ ,  $i = 1, 2, \dots, N_1$ ,  $j = 1, 2, \dots, N_2$ ,  $k = 1, 2, \dots, N_3$ . Let the one-dimensional cutoff functions in  $z$  direction be

$$\mu_{\circlearrowleft, k}^{(3)}(x_1) = \begin{cases} H(\zeta_i - x_3), & \circlearrowleft = -1, \\ H(x_3 - \zeta_{i+1}), & \circlearrowleft = 1, \end{cases}$$

and the cutoff functions for each subdomain be

$$\mu_{i,j,k} = \mu_{-1,i}^{(1)}(x_1)\mu_{+1,i}^{(1)}(x_1)\mu_{-1,j}^{(2)}(x_2)\mu_{+1,j}^{(2)}(x_2)\mu_{-1,k}^{(3)}(x_3)\mu_{+1,k}^{(3)}(x_3). \quad (57)$$

Denote by  $G_{i,j,k}(x, y)$  the fundamental solution of the problem  $\mathcal{P}_{\Omega_{i,j,k}}$ , and let the six boundaries  $\gamma_{\square, \Delta, \bigcirc; i, j, k}$ ,  $(\square, \Delta, \bigcirc) = (\pm 1, 0, 0)$ ,  $(0, \pm 1, 0)$ ,  $(0, 0, \pm 1)$ , of  $\Omega_{i,j,k}$  be

$$\gamma_{\square, \Delta, \bigcirc; i, j, k} = \begin{cases} \{(x_1, x_2, x_3) | x_1 = \xi_i\}, & \text{if } (\square, \Delta, \bigcirc) = (-1, 0, 0) \text{ and } i > 1 \\ \{(x_1, x_2, x_3) | x_1 = \xi_{i+1}\}, & \text{if } (\square, \Delta, \bigcirc) = (+1, 0, 0) \text{ and } i < N_1 \\ \{(x_1, x_2, x_3) | x_2 = \eta_j\}, & \text{if } (\square, \Delta, \bigcirc) = (0, -1, 0) \text{ and } j > 1 \\ \{(x_1, x_2, x_3) | x_2 = \eta_{j+1}\}, & \text{if } (\square, \Delta, \bigcirc) = (0, +1, 0) \text{ and } j < N_2 \\ \{(x_1, x_2, x_3) | x_3 = \eta_k\}, & \text{if } (\square, \Delta, \bigcirc) = (0, 0, -1) \text{ and } k > 1 \\ \{(x_1, x_2, x_3) | x_3 = \eta_{k+1}\}, & \text{if } (\square, \Delta, \bigcirc) = (0, 0, +1) \text{ and } k < N_3 \\ \emptyset, & \text{otherwise,} \end{cases}$$

and the normal direction associated with them be  $\mathbf{n}_{\square, \Delta, \bigcirc} = -(\square, \Delta, \bigcirc)$ . Then the trace operators are defined as

$$\Psi_{\square, \Delta, \bigcirc; i, j, k}(v) := \int_{\gamma_{\square, \Delta, \bigcirc; i, j, k}} J_{i, j, k}^{-1} G_{i, j, k}(x, y) (A_{i, j, k} \nabla_y v(y) \cdot \mathbf{n}_{\square, \Delta, \bigcirc}) \quad (58)$$

$$- v(y) \left( A_{i, j, k} \nabla_y \left( J_{i, j, k}^{-1} G_{i, j, k}(x, y) \right) \cdot \mathbf{n}_{\square, \Delta, \bigcirc} \right) dy \quad (59)$$

where  $J_{i, j, k} = J_{\Omega_{i, j, k}}$ ,  $A_{i, j, k} = A_{\Omega_{i, j, k}}$  and  $(\square, \Delta, \bigcirc) = (\pm 1, 0, 0), (0, \pm 1, 0), (0, 0, \pm 1)$ .

Eight diagonal directions, namely  $(\square, \Delta, \bigcirc)$ ,  $\square, \Delta, \bigcirc = \pm 1$ , are used in 3D diagonal sweeping, and the sweep along each direction contains a total of  $N_1 + N_2 + N_3 - 2$  steps. The sweeping order is the same with [26], i.e.,

$$\begin{aligned} (+1, +1, +1), \quad & (-1, +1, +1), \quad (+1, -1, +1), \quad (-1, -1, +1), \\ (+1, +1, -1), \quad & (-1, +1, -1), \quad (+1, -1, -1), \quad (-1, -1, -1). \end{aligned} \quad (60)$$

The similar direction of vectors in  $\mathbb{R}^3$  is defined as in [26]: two vector  $\mathbf{d}_1$  and  $\mathbf{d}_2$  in  $\mathbb{R}^3$  are called in the *similar direction* if  $\mathbf{d}_1 \cdot \mathbf{d}_2 > 0$  and  $\mathbf{d}_1(k) \mathbf{d}_2(k) \geq 0$  for  $k = 1, 2, 3$ , where  $\mathbf{d}_1(k)$  and  $\mathbf{d}_2(k)$  are the  $k$ -th components of  $\mathbf{d}_1$  and  $\mathbf{d}_2$ , respectively. The rules on transferred source in sweeps in  $\mathbb{R}^3$  are also as in [26]:

**Rule 4.1.** (Similar directions in  $\mathbb{R}^3$ ) *A transferred source which is not in the similar direction of one sweep in  $\mathbb{R}^3$ , should not be used in that sweep.*

**Rule 4.2.** (Opposite directions in  $\mathbb{R}^3$ ) *Suppose a transferred source with direction  $\mathbf{d}_{src}$  is generated in one sweep with direction  $\mathbf{d}_1$ , then it should not be used in the later sweep with direction  $\mathbf{d}_2$ , if under any of  $x - y$ ,  $x - z$ ,  $y - z$  plane projections, the projection of  $\mathbf{d}_{src}$  has exactly one zero components and the projections of  $\mathbf{d}_1$  and  $\mathbf{d}_2$  are opposite.*

The diagonal sweeping DDM with trace transfer in  $\mathbb{R}^3$  is stated as follows.

**Algorithm 4.1** (Diagonal sweeping DDM with trace transfer in  $\mathbb{R}^3$ ).

1: Set the sweep order as list (60)

2: Set the local trace of each subdomain for each sweep as  $\mathbf{g}_{\square, \Delta, \bigcirc; i, j, k}^l$ ,  $l = 1, \dots, 8$   
 3: **for** sweep  $l = 1, \dots, 8$  **do**  
 4:   **for** step  $s = 1, \dots, N_1 + N_2 + N_3 - 2$  **do**  
 5:     **for** subdomain  $\Omega_{i, j, k}$  in the step  $s$  of the current sweep **do**  
 6:       If  $f_{i, j, k} \neq 0$ , solve the local solution  $\mathcal{L}_{i, j, k}(u_{i, j, k}^l) = f_{i, j, k}$ ,  
 7:       or else set  $u_{i, j, k}^l = 0$   
 8:     Set  $f_{i, j, k} = 0$   
 8:     Add potentials to the local solution  

$$u_{i, j, k}^l += \sum_{\substack{(\square, \Delta, \bigcirc) = (\pm 1, 0, 0), \\ (0, \pm 1, 0), (0, 0, \pm 1)}} \Psi_{\square, \Delta, \bigcirc; i, j, k}(\mathbf{g}_{\square, \Delta, \bigcirc; i, j, k}^l)$$
9:     Compute new transferred trace  $\left( u_{i, j, k}^l, A_{i, j, k} \nabla u_{i, j, k}^l \cdot \mathbf{n}_{\square, \Delta, \bigcirc} \right)^T \Big|_{\gamma_{\square, \Delta, \bigcirc; i, j, k}}$ ,  $(\square, \Delta, \bigcirc) = (\pm 1, 0, 0), (0, \pm 1, 0), (0, 0, \pm 1)$   
10:    **for** each direction  $(\square, \Delta, \bigcirc) = (\pm 1, 0, 0), (0, \pm 1, 0), (0, 0, \pm 1)$  **do**  
11:      Find the smallest sweep number  $l' \geq l$ , such that the transferred trace could be  
 used in sweep  $l'$ , according to Rule 4.1 and 4.2  
12:      Add the transferred trace to the  $l'$ -th trace of the corresponding neighbor  
 subdomain  

$$\mathbf{g}_{-\square, -\Delta, -\bigcirc; i + \square, j + \Delta, k + \bigcirc}^{l'} += \left( u_{i, j, k}^l, A_{i, j, k} \nabla u_{i, j, k}^l \cdot \mathbf{n}_{\square, \Delta, \bigcirc} \right)^T \Big|_{\gamma_{\square, \Delta, \bigcirc; i, j, k}}$$
13:    **end for**  
14:   **end for**  
15:   **end for**  
16: **end for**  
17: Summarize the DDM solution as

$$u_{DDM} = \sum_{l=1, \dots, 8} \sum_{\substack{i=1, \dots, N_1 \\ j=1, \dots, N_2 \\ k=1, \dots, N_3}} u_{i, j, k}^l \mu_{i, j, k}$$

---

The DDM solution of the above algorithm is exactly the solution to  $\mathcal{P}_\Omega$  with the source  $f$ , in the constant medium case and also the two-layered medium case provided the source lies below medium interface. The verification in the constant medium case is similar to the source transfer case in [26], in fact, it is simplified since only cardinal directions need to be considered with the transferred traces. On the other hand, the verification of the two-layered medium case follows the same line of argument in the  $\mathbb{R}^2$  case. Therefore the verifications of both cases are omitted.

**Remark 2.** *The diagonal sweeping DDM is a highly efficient method in terms of computational complexity and weak scalability. When we increase the number of subdomains while fixing the subdomain problem size, the computational complexity of solving one RHS with Krylov subspace solver using the diagonal sweeping method as a preconditioner becomes  $O(Nn_{iter})$ , where  $N$  is the size of global system and  $n_{iter}$  is the number of iterations of Krylov subspace. If  $n_{iter}$  grows*

proportionally to  $\log N$ , which is to be investigated in the numerical test section, then the method is of  $O(N \log N)$  complexity.

Although the method is sequential, for problems with many RHSs, it is possible to set up a pipeline to solve all the RHSs in sequence, and the average solving time for one RHS in the method is

$$8T_0 n_{iter} \left(1 + \frac{N_1 + N_2 + N_3 - 2}{N_{RHS}}\right), \quad (61)$$

where  $T_0$  is the time cost of one subdomain solve, and  $N_{RHS}$  is number of RHSs. Thus to produce an efficient pipeline, the number of RHSs is only required to be several times of  $N_1 + N_2 + N_3$ . We use the ideal parallel time cost, defined by  $T_{par} := 2^n T_0 n_{iter}$ , to approximate the time cost of our method for one RHS in many RHSs problem, and if  $n_{iter}$  grows proportionally to  $\log N$ , the weak scalability of the method will be quite satisfactory for large scale Helmholtz problem with large wave number.

## 5. Numerical test

The numerical test of the diagonal sweep algorithm with trace transfer is presented in this section. First, the convergence of the algorithm is tested in the following sense. The error of the numerical solution of the DDM consists of errors from the numerical discretization, the truncation of the PML layer and the DDM algorithm, however, in the constant medium case and the two-layered medium case under certain conditions, there is no error from the DDM algorithm. Therefore, using appropriate PML medium parameters to keep the PML truncation error relatively small (which is easy since the truncation error decays exponentially away from the region), the total error will be dominated by the numerical discretization error, which could be checked using the convergence order. Second, the performance of the algorithm is tested as a preconditioner. The DDM solution of the algorithm is an approximate solution to the problem in general case, hence it could be used as a preconditioner for the Krylov subspace method, and the effectiveness of the DDM preconditioner is measured by the iteration number. In the end, we use the algorithm as a preconditioner to solve the 2004 BP model, which is a more complicate problem from real applications.

The finite difference discretization (FD) scheme on the structured mesh is adopted in all the numerical tests, the five points scheme and the seven points scheme are employed in two and three dimensions respectively, both of the schemes are of second order accurate. The mesh density is defined as the number of nodes per wave length, and a minimum mesh density is used to ensure the accuracy of the 2nd order FD scheme. The parallel DDM algorithms are implemented using Message Passing Interface (MPI), and the spare direct solver “MUMPS” [1] are used to solve local subdomain problems. The numerical tests are carried out on the “Lssc-IV” cluster at the State Key Laboratory of Scientific and Engineering Computing, Chinese Academy of Sciences, each node of the cluster has two 2.3GHz Xeon Gold 6140 processors with 18 cores, and 192G shared memory.

### 5.1. Convergence tests of the discrete DDM solutions

In this subsection, the convergence of the proposed algorithm is tested in the constant medium case and the two-layered medium case. The error of the DDM solution is expected to be dominated by the discretization error, hence we fixed both the wave number and the number of subdomains, and increase the mesh resolution to check the convergence order.

### 5.1.1. 2D example of constant medium

A 2D constant medium problem is used to test the proposed Algorithm 2.1. The computational domain is  $B_L = [0, 2L] \times [0, 2L]$  with  $L = 1/2$ , and the interior domain without PML is  $B_l = [0, 2l] \times [0, 2l]$  with  $l = 25/56$ . For the wave number  $k = 50\pi$ , a series of uniformly refined meshes is used, of which the mesh density increases approximately from 11 to 173. The domain partition is fixed to be  $4 \times 4$  for all the meshes, and the source is defined as,

$$f(x_1, x_2) = \frac{16k^2}{\pi^3} e^{-\left(\frac{4k}{\pi}\right)^2((x_1-r_1)^2+(x_2-r_2)^2)},$$

where  $(r_1, r_2) = (0.28, 0.27)$ , such that it is supported in four subdomains  $\Omega_{i,j}$ ,  $i = 1, 2$ ,  $j = 1, 2$ .

The optimal second order convergence of the errors in  $L^2$  and  $H^1$  norms along the mesh refinement are obtained, as is reported in Table 1, which implies the total error is indeed dominated by the 2nd order finite difference discretization error in the constant medium case. The results of the algorithm with trace and source transfer are very close to each other, the differences in error are in the fourth digits, hence they are not shown in the table.

Mesh Size	Local Size without PML	$L^2$ Error	Conv. Rate	$H^1$ Error	Conv. Rate
$270^2$	$60^2$	$1.38 \times 10^{-2}$		$2.13 \times 10^0$	
$540^2$	$120^2$	$3.43 \times 10^{-3}$	2.0	$5.35 \times 10^{-1}$	
$1080^2$	$240^2$	$8.51 \times 10^{-4}$	2.0	$1.33 \times 10^{-1}$	2.0
$2160^2$	$480^2$	$2.12 \times 10^{-4}$	2.0	$3.33 \times 10^{-2}$	2.0
$4320^2$	$960^2$	$5.30 \times 10^{-5}$	2.0	$8.32 \times 10^{-3}$	2.0

Table 1: The errors and convergence rates of the solutions of proposed DDM for the constant medium problem in  $\mathbb{R}^2$ .

### 5.1.2. 2D example of two-layered medium

Next we test the Algorithm 2.1 with the Helmholtz problem in  $\mathbb{R}^2$  using the same setting as the first example, except that the wave number is changed. The two-layered medium profile is chosen as follows,

$$k = \begin{cases} k_2 & x_2 > \eta_L + \varepsilon \\ k_1(1-w) + k_2 w & \eta_L \leq x_2 \leq \eta_L + \varepsilon \\ k_1 & x_2 < \eta_L \end{cases}$$

where  $k_1 = 50\pi$ ,  $k_2 = 62.5\pi$ ,  $\eta_L = 0.65$  and  $\varepsilon = 0.01$ , so that the wave number changes from  $k_1$  to  $k_2$  in a thin layer with width  $\varepsilon$ , as is shown in Figure 10 (a). The real part of the discrete DDM solution on the mesh of  $1080^2$  is shown in Figure 10 (b), the optimal second order convergence of the errors in  $L^2$  and  $H^1$  norms along the mesh refinement are obtained, as is shown in Table 2, which implies the total error is indeed dominated by the 2nd order finite difference discretization error in the two-layered medium case. Again the result of the algorithm with trace and source transfer are very close to each other and not shown in the table.

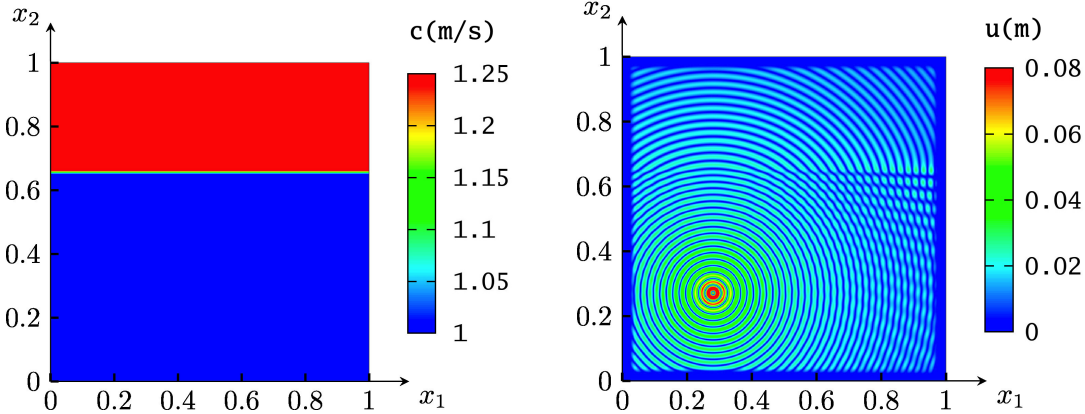


Figure 10: Velocity profile (left) and the real part of the DDM solution (right) of the 2D two-layered medium.

Mesh Size	Local Size without PML	$L^2$ Error	Conv. Rate	$H^1$ Error	Conv. Rate
$270^2$	$60^2$	$1.37 \times 10^{-2}$		$1.97 \times 10^0$	
$540^2$	$120^2$	$3.39 \times 10^{-3}$	2.0	$4.91 \times 10^{-1}$	2.0
$1080^2$	$240^2$	$8.41 \times 10^{-4}$	2.0	$1.22 \times 10^{-1}$	2.0
$2160^2$	$480^2$	$2.10 \times 10^{-4}$	2.0	$3.05 \times 10^{-2}$	2.0
$4320^2$	$960^2$	$5.25 \times 10^{-5}$	2.0	$7.63 \times 10^{-3}$	2.0

Table 2: The errors and convergence rates of the solutions of proposed DDM for the two-layered medium problem in  $\mathbb{R}^2$ .

### 5.2. Performance tests with the DDM as a preconditioner in $\mathbb{R}^2$

The DDM Algorithm 2.1 is then tested as a preconditioner for solving the discrete linear system of the Helmholtz problem in the constant medium and multi-layered medium case, where each preconditioner solving consists four diagonal sweeps, and each sweep has  $N_1 + N_2 - 1$  sequential steps. The effectiveness and efficiency of the proposed method as preconditioner are tested for the increasing number of subdomains and frequencies, while the subdomain problem size and mesh density is fixed. The performance of the proposed method is also compared to the diagonal sweeping method with source transfer. In all the tests, the stopping criteria is that the relative residual is less than  $10^{-8}$ .

#### 5.2.1. Constant medium problem

The proposed method is tested in a constant medium problem on the square domain  $[0, 1] \times [0, 1]$  with a series of uniformly refined meshes. The source contains four approximated delta sources, that is

$$f(x_1, x_2) = \sum_{\substack{i=1, \dots, N_x \\ j=1, \dots, N_y}} \sum_{s=1, \dots, 4} \frac{1}{h_1 h_2} \delta(x_1^s - ih_1) \delta(x_2^s - jh_2), \quad (62)$$

where  $(x_1^s, x_2^s) = (1/4, 1/4), (1/4, 3/4), (3/4, 1/4)$  and  $(3/4, 3/4)$ , for  $s = 1, \dots, 4$ , and  $h_1$  and  $h_2$  are the grid spacing in  $x$  and  $y$  direction, respectively. The frequencies and number of subdomain

increases as the mesh resolution increase, while the size of the subdomain problems is fixed to be  $300 \times 300$ , and the mesh density is kept 10. The PML layer is of 30 points, which is of 3 wave length.

The results of the diagonal sweeping method for both source transfer and trace transfer are reported in Table 3. As we can see, both the GMRES iterative steps (denoted by  $n_{\text{iter}}$ ) and the ideal parallel solving time grows roughly proportionally to  $\log(N_1 + N_2)$  or  $\log(\omega)$ , which shows that the solvers with both transfer methods are highly efficient. It is also shown in the table that the performance of the diagonal sweeping DDMs with different transfer method are very close using the 2nd order finite difference discretization, in particular, the GMRES iterative steps are the same with two methods.

Mesh Size	$N_1 \times N_2$	Freq. $\omega/2\pi$	Source transfer			Trace transfer		
			GMRES $n_{\text{iter}}$	$T_{\text{it}}$	$T_{\text{par}}$	GMRES $n_{\text{iter}}$	$T_{\text{it}}$	$T_{\text{par}}$
$600^2$	$2 \times 2$	65.9	3	32.0	10.7	3	29.3	9.8
$1200^2$	$4 \times 4$	126	3	73.8	10.5	3	64.4	9.2
$2400^2$	$8 \times 8$	246	3	136	9.1	3	124	8.2
$4800^2$	$16 \times 16$	486	3	286	9.2	3	268	8.7
$9600^2$	$32 \times 32$	966	4	766	12.2	4	715	11.4

Table 3: The performance of the proposed DDM as an iterative solver for the 2D constant medium problem with the subdomain problem size being fixed.

### 5.2.2. Layered medium problem

The proposed method is then tested in a multi-layered medium problem on the square domain  $[0, 1] \times [0, 1]$  with a series of uniformly refined meshes, the medium consists of five titled layers, where the largest value of velocity is twice of the smallest, as shown in Figure 11. The source (62) is used again, and the series of uniformly refined mesh and domain partition are the same the previous test. The frequencies increase as the mesh refines, while the minimum mesh density is kept to be 10.

The results of the diagonal sweeping methods with both transfer methods are reported in Table 4. The performances of the diagonal sweeping DDMs with different transfer methods are very close again. Compare to the constant medium test, the GMRES iterative steps are larger in this multi-layered medium test, since the convergence rate is limited by the reflection rate of the layer interfaces [26]. Both the GMRES iterative steps and the ideal parallel solving time grows roughly proportionally to  $\log(N_1 + N_2)$  or  $\log(\omega)$ , which demonstrates the efficiency of the proposed method.

### 5.3. The BP-2004 model

At last, the performance of the proposed method is tested with the 2D BP-2004 velocity model [23], which is a popular benchmark problem in seismic exploration to study reverse time migration. The middle part of the model that contains the slat body is used, which is 24km in length and 12km in depth, and the velocity range is  $[1, 5]$  km/s, as is shown in Figure 12. A delta source locates at  $((\frac{N_1}{2} + \frac{1}{3})\Delta\xi, -\frac{1}{3}\Delta\eta)$  is chosen as the source function. A series of uniformly refined mesh is used, and the domain is partitioned into subdomain that always containing  $300 \times 300$  grid points without

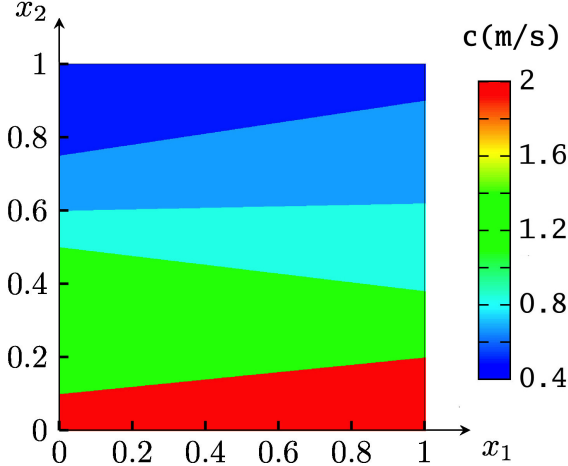


Figure 11: Velocity profile of the 2D five-layered medium problem.

Mesh Size	$N_1 \times N_2$	Freq. $\omega/2\pi$	Source transfer			Trace transfer		
			GMRES $n_{\text{iter}}$	$T_{\text{it}}$	$T_{\text{par}}$	GMRES $n_{\text{iter}}$	$T_{\text{it}}$	$T_{\text{par}}$
$600^2$	$2 \times 2$	33	6	56.3	18.8	6	51.4	17.1
$1200^2$	$4 \times 4$	63	8	160	22.9	8	145	20.7
$2400^2$	$8 \times 8$	123	8	298	19.9	8	273	18.2
$4800^2$	$16 \times 16$	243	9	701	22.6	9	650	21.0
$9600^2$	$32 \times 32$	483	10	1678	26.6	10	1556	24.7

Table 4: The performance of the diagonal sweeping DDM as a preconditioner for the 2D five-layered medium problem with the subdomain problem size being fixed.

PML. The frequencies increase as the mesh refines, while the minimum mesh density is kept to be 10.

The discrete solution with the frequency  $\omega/2\pi = 14.6$  is shown in Figure 13, and the performance results of diagonal sweeping method with both transfer methods are reported in Table 5. Again the performances of the diagonal sweeping DDMs with different transfer methods are very close. The GMRES iterative steps are even larger in this case compared to the five-layered medium case in the previous subsection, since the medium profile is more complicated, nevertheless, both the GMRES iterative steps and the ideal parallel solving time still grows roughly proportionally to  $\log(N_1 + N_2)$  or  $\log(\omega)$ , which shows that the proposed method is effective and highly efficient for real applications.

## 6. Conclusions

In this paper, the diagonal sweeping DDM is re-proposed with trace transfer method, the overlapping subdomain decomposition is relaxed to be non-overlapping, and less number of directions of transferred solution information is required, which makes the new proposed method more efficient than its counterpart with source transfer. We proved that the proposed method forms the exact solution in the constant medium case, and also the two-layered medium case under certain

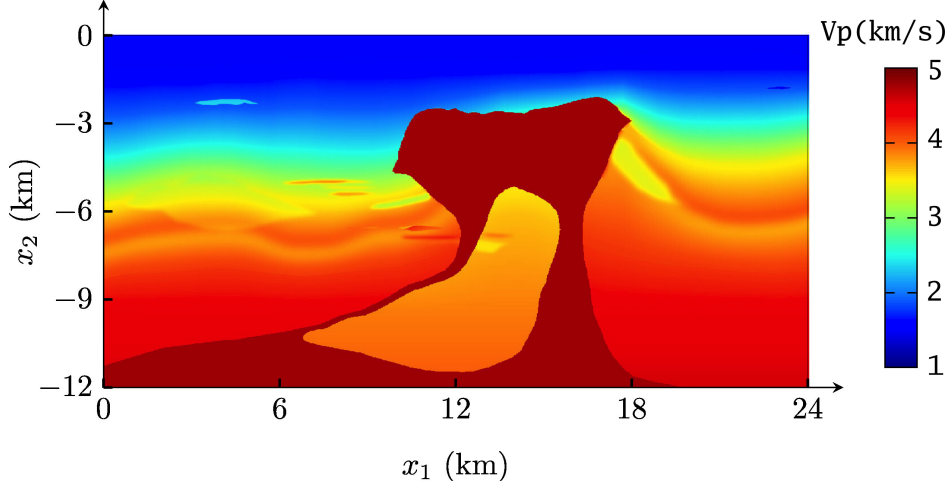


Figure 12: The velocity profile of the BP-2004 model.

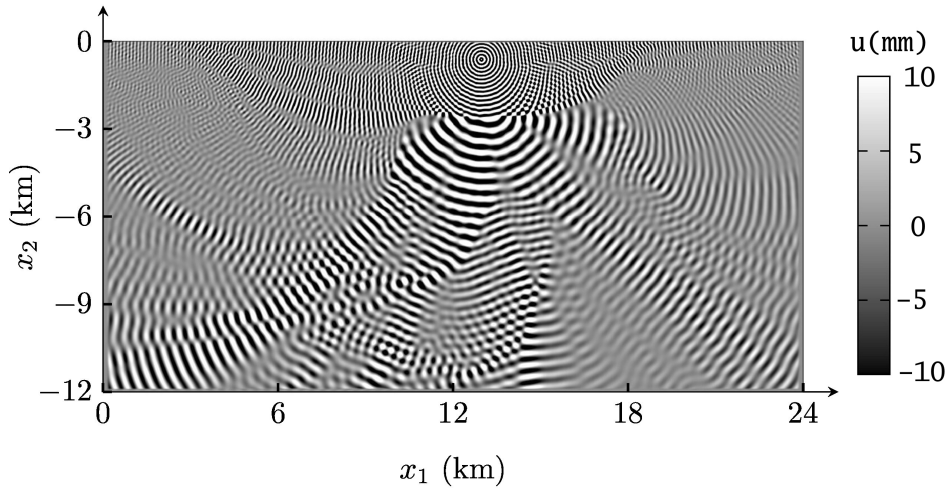


Figure 13: The real part of the approximate DDM solution of the BP-2004 model on the mesh of size  $2400 \times 1200$ .

Mesh Size	$N_1 \times N_2$	Freq. $\omega/2\pi$	Source transfer			Trace transfer		
			GMRES $n_{\text{iter}}$	$T_{\text{it}}$	$T_{\text{par}}$	GMRES $n_{\text{iter}}$	$T_{\text{it}}$	$T_{\text{par}}$
$600^2$	$2 \times 2$	3.9	6	54.9	18.3	6	46.9	15.6
$1200^2$	$4 \times 4$	7.5	7	145	20.7	7	128	18.3
$2400^2$	$8 \times 8$	14.6	8	305	20.3	8	274	18.2
$4800^2$	$16 \times 16$	28.9	10	775	25.0	10	713	23.0
$9600^2$	$32 \times 32$	57.5	11	1844	29.3	11	1681	26.7

Table 5: The performance of the diagonal sweeping DDM as a preconditioner for the BP-2004 problem with the subdomain problem size being fixed.

conditions, which lays down the theoretical foundation of the method. The implementation of

higher order discretizations for the diagonal sweeping method with source transfer is quite straight forward, while the implementation of the DDM with trace transfer requires more investigation, for example, the high order numerical quadrature for the potential computation with the singular integrand need to be developed, and the special treatment of the quadrature around the crossing of subdomain interfaces need to be found. The PML boundary for sweeping DDM has been shown to be effective, however, the absorption deteriorates for the near-grazing incident waves that come from the source near the boundary, which may cause the sweeping DDM less effective. Another difficulty involving PML emerges when extending the method to Maxwell's equation and the elastic equation, that is, the required number of grid points in the PML is too many to reach satisfactory absorption effect, which brings too much extra computation in the subdomain problem. Therefore, the development of more effective PML is another vital direction of our future research. The optimization of the proposed method follows the same line with its counterpart with source transfer, where the pipeline setup, parallel computing strategy, and sparse direct solver need to be carefully designed and implemented, which is another direction of our future research.

## References

- [1] P.R. Amestoy, I.S. Duff, J. Koster and J.Y. L'Excellent. A fully asynchronous multifrontal solver using distributed dynamic scheduling. *SIAM J. Matrix Anal. Appl.*, 23(1):15-41, 2001.
- [2] D. Aruliah and U. Ascher. Multigrid preconditioning for Krylov methods for time-harmonic Maxwell's equations in three dimensions. *SIAM Journal on Scientific Computing*, 24(2):702718, 2002.
- [3] J.P. Berenger. A perfectly matched layer for the absorption of electromagnetic waves. *J. Comput. Phys.*, 114(2):185-200, 1994.
- [4] Y. Boubendir, X. Antoine, and C. Geuzaine. A quasi-optimal nonoverlapping domain decomposition algorithm for the Helmholtz equation. *Journal of Computational Physics*, 231(2):262-280, 2012.
- [5] J.H. Bramble and J.E. Pasciak. Analysis of a cartesian PML approximation to acoustic scattering problems in  $R^2$  and  $R^3$ , *J. Comput. Math.*, 247:209-230, 2013.
- [6] Z. Chen and W. Zheng. Convergence of the uniaxial perfectly matched layer method for time-harmonic scattering problems in two-layered media. *SIAM J. Numer. Anal.*, 48(6):2158-2185, 2010.
- [7] Z. Chen and X. Xiang. A source transfer domain decomposition method for Helmholtz equations in unbounded domain. *SIAM J. Numer. Anal.*, 51(4):2331-2356, 2013.
- [8] W.C. Chew and W.H. Weedon. A 3D perfectly matched medium from modified Maxwell's equations with stretched coordinates. *Microw. Opt. Techn. Let.*, 7(13):599-604, 1994.
- [9] F. Collino, S. Ghanemi, and P. Joly. Domain decomposition method for harmonic wave propagation: a general presentation. *Computer Methods in Applied Mechanics and Engineering*, 184(24):171-211, 2000.

- [10] B. Després. Décomposition de domaine et problème de Helmholtz. *Comptes rendus de l'Académie des sciences, Série 1, Mathématique*, 311:313-316, 1990.
- [11] J. Douglas, Jr. and D. B. Meade. Second-order transmission conditions for the Helmholtz equation, in Ninth International Conference on Domain Decomposition Methods, P. E. Bjorstad, M. S. Espedal, and D. E. Keyes, eds., DDM.org, pages 434-441, 1998.
- [12] Y. Du and H. Wu. An improved pure source transfer domain decomposition method for Helmholtz equations in unbounded domain. ArXiv preprint, arXiv:1505.06052, 2015.
- [13] I.S. Duff and J. Reid, The multifrontal solution of indefinite sparse symmetric linear equations, *ACM Trans. Math. Soft.*, 9:302-325, 1983.
- [14] B. Engquist and L. Ying. Sweeping preconditioner for the Helmholtz equation: hierarchical matrix representation. *Comm. Pure Appl. Math.*, 64(5):697-735, 2011.
- [15] B. Engquist and L. Ying. Sweeping preconditioner for the Helmholtz equation: moving perfectly matched layers. *Multiscale Model. Simul.*, 9(2):686-710, 2011.
- [16] B. Engquist, H. Zhao. Approximate Separability of the Green's Function of the Helmholtz Equation in the High Frequency Limit. *Communications on Pure and Applied Mathematics*, 71(1), 2016.
- [17] Y.A. Erlangga , C. Vuik , C.W. Oosterlee. Comparison of multigrid and incomplete LU shifted-Laplace preconditioners for the inhomogeneous Helmholtz equation. *Applied Numerical Mathematics*, 56(5):648-666, 2006.
- [18] Y.A. Erlangga , R. Nabben. On a multilevel Krylov method for the Helmholtz equation preconditioned by shifted Laplacian. *Electronic Transactions on Numerical Analysis Etna*, 21(539):396, 2008.
- [19] Y.A. Erlangga, C.W. Oosterlee, and C. Vuik. A novel multigrid based preconditioner for heterogeneous Helmholtz problems. *SIAM Journal on Scientific Computing*, 27(4):14711492, 2006.
- [20] M Gander, H. Zhang. A class of iterative solvers for the Helmholtz equation: Factorizations, sweeping preconditioners, source transfer, single layer potentials, polarized traces, and optimized Schwarz methods, *SIAM Rev.*, to appear.
- [21] M. Gander. Optimized Schwarz methods. *SIAM J. Sci. Comput.*, 44(2):699-731, 2006.
- [22] A. George. Nested dissection of a regular finite element mesh. *SIAM Journal on Numerical Analysis*, 10:345363, 1973.
- [23] F. J., Billette and Brandsberg-Dahl Sverre. The 2004 BP velocity benchmark. 67th EAGE Conference & Exhibition, 2005.
- [24] S. Kim and J.E. Pasciak, Analysis of a cartesian PML approximation to acoustic scattering problems in  $\mathbb{R}^2$ , *J. Math. Anal. Appl.*, 370:168-186, 2010.

- [25] W. Leng and L. Ju. An Additive overlapping domain decomposition method for the Helmholtz equation. *SIAM J. Sci. Comput.*, 41(2), A1252A1277, 2019.
- [26] W. Leng and L. Ju. A diagonal sweeping domain decomposition method for the Helmholtz Equation. *ArXiv preprint*, arXiv:2002.05327, 2020.
- [27] M. Lassas and E. Somersalo. Analysis of the PML equations in general convex geometry. *Proc. Roy. Soc. Eding.* 131, 1183-1207, 2001.
- [28] F. Liu and L. Ying. Recursive sweeping preconditioner for the 3D Helmholtz equation. *SIAM J. Sci. Comput.*, 38(2), A814-A832, 2016.
- [29] A. Sch  adle and L. Zschiedrich. Additive Schwarz method for scattering problems using the PML method at interfaces, in *Domain Decomposition Methods in Science and Engineering XVI*, O. Widlund and D. E. Keyes, eds., Heidelberg, Springer-Verlag, page 205-212, 2007.
- [30] A.H. Sheikh, D. Lahaye, and C. Vuik. On the convergence of shifted Laplace preconditioner combined with multilevel deflation. *Numerical Linear Algebra with Applications*, 20(4):645662, 2013.
- [31] C.C. Stolk. A rapidly converging domain decomposition method for the Helmholtz equation. *J. Comput. Phys.*, 241:240-252, 2013.
- [32] M. Taus, L. Zepeda-N  ez, R. J. Hewett, and L. Demanet. L-Sweeps: A scalable, parallel preconditioner for the high-frequency Helmholtz equation. *ArXiv preprint*, arXiv:1909.01467, 2019.
- [33] A. Toselli, Overlapping methods with perfectly matched layers for the solution of the Helmholtz equation, in *Eleventh International Conference on Domain Decomposition Methods*, C. Lai, P. BJORSTAD, M. Cross, and O. Widlund, eds., DDM.org, pages 551-558, 1999.
- [34] N. Umetani, S. P. MacLachlan, and C. W. Oosterlee, A multigrid-based shifted laplacian preconditioner for a fourth-order helmholtz discretization, *Numerical Linear Algebra with Applications*, 16:603626, 2009.
- [35] A. Vion and C. Geuzaine. Double sweep preconditioner for optimized Schwarz methods applied to the Helmholtz problem. *J. Comput. Phys.*, 266:171-190, 2014.
- [36] J. Xia, S. Chandrasekaran, M. Gu, and X. S. Li. Superfast multifrontal method for large structured linear systems of equations. *SIAM Journal on Matrix Analysis and Applications*, 31(3):13821411, 2010.
- [37] L. Zepeda-N  ez and L. Demanet. The method of polarized traces for the 2D Helmholtz equation. *J. Comput. Phys.*, 308:347-388, 2016.